UNIVERSITÀ DEGLI STUDI DELL'INSUBRIA
Dipartimento di Biotecnologie e Scienze della Vita

Dottorato di Ricerca in
Medicina Sperimentale e Traslazionale
Curriculum: Neuroscienze

Ph.D. Thesis of
Marco Tramarin

Critical role of CDKL5 in AMPA receptor composition: underlying mechanism and functional outcome

Ph.D. Coordinator: Prof. Daniela Negrini
Supervisor: Prof. Charlotte Kilstrup-Nielsen

Ph.D. Course XXIX Cycle 2014-2017

"We are a way for the Cosmos to know itself"

Carl Sagan

TABLE OF CONTENTS

1. ABSTRACT **5**

2. INTRODUCTION **6**

2.1 CDKL5 disorder: from the discovery of the gene to the characterization of the disease 6

2.2 CDKL5/Cdkl5 gene, isoforms and their expression in brain 7

2.3 CDKL5 protein 9

2.4 CDKL5 pathological variants 10

2.5 Roles of CDKL5 in synaptic function, morphology and plasticity 12

2.6 AMPA receptor structure and subunit composition 14

2.7 Biophysical and molecular properties of AMPA receptors 15

2.8 AMPA receptor-interacting proteins 16

2.8.1 NTD-interacting proteins 16

2.8.2 CTD-interacting proteins 17

2.9 AMPA receptor biosynthesis and trafficking 19

2.10 AMPAR trafficking in LTP and LTD 20

2.11 AMPAR subunits and disease 22

3. RESULTS **23**

3.1 CDKL5 knock-down differentially affects the expression level of AMPA receptor subunits 23

3.2 Altered expression of GluA2 subunit in Cdkl5-silenced neurons rely on post-transcriptional mechanisms 25

3.3 Cdkl5 knock-down results in increased GluA2 phosphorylation at Serine 880 26

3.4 Cdkl5-silencing drives internalized GluA2-containing AMPARs to lysosomal degradation 27

3.5 Cdkl5 knock-out neurons and adult hippocampus recapitulate the biochemical alterations of AMPA receptor observed in Cdkl5-silenced cultures 29
3.6 Cdkl5 knock-down impairs membrane exposure of GluA2-containing AMPA receptors 31
3.7 Cell-surface biotinylation assays confirm defective AMPAR expression in Cdkl5-silenced neuronal cultures 33
3.8 Calcium imaging reveals an increased calcium influx through AMPARs in Cdkl5-deficient neurons 35
3.9 Cdkl5 silencing alters spine number and morphology 37
3.10 Wild type CDKL5, but not pathological mutants, promotes surface expression of homomeric GluA2 AMPA receptors in COS7 cells 39
3.11 GRASP-1 is a novel interactor of CDKL5 41
3.12 The phosphorylation status of GRASP-1 changes during brain development 43
3.13 Tianeptine normalizes GluA2 subunit expression and S880 phosphorylation in Cdkl5-deficient cultures 44

4. DISCUSSION 46

4.1 CDKL5 knock-down affects GluA2 expression and subunit composition of membrane-inserted AMPARs 46
4.2 CDKL5 is involved in molecular pathways that regulate the membrane insertion and recycling of GluA2-containing AMPARs 49
4.3 Tianeptine is a promising drug for CDKL5-associated AMPAR defects 53
4.4 Conclusions 55

5. EXPERIMENTAL PROCEDURES 56

6. ACKNOWLEDGEMENTS 64

7. REFERENCES 65

1. ABSTRACT

Neurological disorders associated with the X-linked kinase CDKL5 are characterized by the early onset of seizures, severe cognitive deficits and autistic traits. No curative therapy exists for these patients and treatments are only focused on alleviating symptoms. Loss of Cdkl5 affects spine density and stabilization as well as synaptic activity, but the underlying molecular mechanisms are still far from fully understood.

Here we show several pieces of evidence linking Cdkl5-associated synaptic defects to AMPA receptor (R) expression and subunit composition. In particular, primary hippocampal neurons devoid of Cdkl5 have defective GluA2-subunit expression, as well as a hyper-phosphorylation of Serine 880 (S880). Moreover, Cdkl5-downregulation skews the composition of membrane-inserted AMPARs towards the GluA2-depleted calcium-permeable form. The depletion of membrane-inserted GluA2 is likely to rely on defective recycling. Indeed, at the molecular level, we find that CDKL5 interacts with GRASP-1, a neuron-enriched protein that coordinates the endosomal sorting of AMPARs towards the plasma membrane. Against this background, we assume that the resulting alterations can underlie, at least in part, the synaptic dysfunctions and cognitive deficits in CDKL5 disorder. Finally, we provide evidence that tianeptine, a promising drug previously reported to modulate AMPAR-mediated glutamatergic neurotransmission, is capable of restoring GluA2 expression and S880 phosphorylation in neurons devoid of CDKL5. These results places tianeptine as an interesting candidate drug for CDKL5-disorder, the therapeutic potential of which will be further investigated.

2. INTRODUCTION

2.1 CDKL5 disorder: from the discovery of the gene to the characterization of the disease

The Cyclin-Dependent Kinase-Like 5, CDKL5 (Mendelian Inheritance in Man, MIM: 300203), was identified in 1998 by Montini and colleagues (*1*) through positional cloning studies aimed to isolate disease genes located in Xp22 where a number of human genetic disorders had formerly been mapped including Nance-Horan (NH) syndrome, oral–facial–digital syndrome type 1 (OFD1) and nonsyndromic sensorineural deafness (DFN6).

Since CDKL5 sequence analysis revealed homologies to several serine-threonine kinases, the protein was initially named STK9 (Serine Threonine Kinase 9) but, after sequence comparisons, the *STK9* gene was renamed *CDKL5* because of the strong similarity to cyclin-dependent kinases (*2*).

In 2003, Vera Kalscheuer linked chromosomal rearrangements involving *CDKL5* with severe intellectual disability and early onset seizures (*2*). In the following year, different *CDKL5* mutations were described in individuals with infantile spasms, mental retardation and clinical manifestation similar to Rett syndrome (RTT) (*3*, *4*); *CDKL5* was thus proposed as a novel gene implicated in the "early seizure variant" of RTT, also known as the Hanefeld variant in honor of the physician who described it for the first time in 1985 (*5*).

At first, screenings for *CDKL5* mutations were focused on cohorts of female patients with a clinical phenotype mimicking RTT, which is in most cases caused by mutations in the X-linked *MECP2* gene. Many of the early-onset encephalopathies have overlapping phenotypes (*6*, *7*). Some are distinctive either by dysmorphism or typical neurodevelopmental profile, but others, including CDKL5 disorder, at first may be less easily recognized, which is why they were classified as "variant" of others syndromes. To date, studies performed on a larger number of individuals with CDKL5 disorder have better characterized the spectrum of clinical presentations and confirmed that this disease is an independent clinical entity (*8*, *9*). Clinical features characterizing CDKL5 disorder include early-onset seizures (generally appearing within 3 months of life), severe global developmental delay, abnormal muscle tone, hand stereotypies, gastrointestinal problems and bruxism (Table 1) (*8*). Moreover,

subtle but shared dysmorphic features have also been described in individuals with a CDKL5 mutation such as a prominent/broad forehead, deep-set but large-appearing eyes, full lips and tapered fingers; these traits can be useful for clinicians in determining whether the patient warranted CDKL5-specific mutation testing. Variability in clinical features has also been reported since some individuals are less severely affected in terms of motor skills and expressive communication (*10*, *11*). Those differences can be partially due to X-inactivation, resulting in a mosaic expression of normal and mutant CDKL5 protein. As a matter of fact, males with *CDKL5* mutations tend to be more severely affected than females.

Extremely likely (>90% of cases)	• Seizures within the first year of life (90% by 3 months) • Global developmental delay • Severely impaired gross motor function
Very likely (80-90% of cases)	• Sleep disturbances • Abnormal muscle tone • Bruxism • Gastrointestinal issues
Likely (40-80% of cases)	• Subtle dysmorphic features including three or more of the following: broad/prominent forehead; large 'deep-set' eyes; full lips; tapered fingers; and anteverted nares in males • Hand stereotypies • Laughing and screaming spells • Cold hands or feet • Breathing disturbances • Peripheral vasomotor disturbances
Unlikely (<10 % of cases)	• Independent walking • Microcephaly • Major congenital malformations

Table 1| Clinical features suggesting a diagnosis of the CDKL5 disorder according to (*8*).

2.2 *CDKL5/Cdkl5 gene,* isoforms and their expression in brain

The knowledge of *CDKL5* transcripts and isoforms and their developmental expression profile is essential for understanding the mechanistic roles of the kinase in brain development. Since the discovery of the *CDKL5* gene, the characterization of its transcripts and the resulting protein isoforms remained incomplete; however, recently Hector and colleagues (*12*) systematically outlined human *CDKL5* and mouse *Cdkl5* mRNA products and predicted the protein isoform translated from each transcript (Table 2).

According to the current knowledge, the human *CDKL5* gene occupies approximately 240 kb of the Xp22 region and is composed of 24 exons and its expression comprises five major transcript isoforms: *hCDKL5_1-5*. Consistent with a previous publication (*13*), *hCDKL5_1* (formerly known as $CDKL5_{107}$) appears to be the most abundant transcript in the CNS, while *hCDKL5_2-4* represent less than 15% of *CDKL5* transcripts expressed in the whole brain and *hCDKL5_5* (formerly $CDKL5_{115}$), in the adult, is only detected in testis. The murine transcript *mCdkl5_1* appears to be completely orthologous to its human counterpart and is also the most abundant *Cdkl5* transcript in mouse brain.

Analyses of human transcript expression profiles during development revealed that *hCDKL5_1-4* are expressed at higher levels in the adult than in the foetal brain. Conversely, *hCDKL5_5*, which, in the adult, is expressed only in testis, is, however, expressed in foetal human brain. The expression of *Cdkl5* across a developmental time series revealed that *mCdkl5_1* and *mCdkl5_2* are expressed throughout murine brain development, increasing in levels and peaking within the first few postnatal weeks, with *mCdkl5_1* expressed at higher levels than *mCdkl5_2* as previously noted.

Isoform nomenclature		Coding region sizes		
Human	**Mouse**	**(bp)**	**(aa)**	**Former name**
hCDKL5_1	*mCdkl5_1*	2883	960	$CDKL5_{107}$
hCDKL5_2	*mCdkl5_2*	3006	1001	CDKL5-16b
hCDKL5_3		2832	943	-
hCDKL5_4		2955	984	-
hCDKL5_5		3093	1030	$CDKL5_{115}$
	mCdkl5_6	2769	923	-
	mCdkl5_7	2796	931	-
	mCdkl5_8	2817	938	$CDKL5_{105}$

Table 2| Summary of *CDKL5/Cdkl5* isoforms and nomenclature (*12*).

A detailed analysis of *Cdkl5* expression in adult mouse brain showed that its mRNA is particularly abundant in the forebrain. In particular, higher expression levels are detected in most superficial cortical layers involved in the intercortical connectivity. Interestingly, *Cdkl5* mRNA expression is more evident in the frontal cortex, motor cortex and cingulate gyrus,

suggesting the involvement of CDKL5 in mental diseases related to the physiological role of these areas. Moreover, high expression levels are detected also in all CA fields of hippocampus and in the entorhinal cortex pointing out that CDKL5 might be involved in higher cognitive functions like learning and memory. Looking at the cellular level, *Cdkl5* transcripts seem to be expressed mostly in glutamatergic and GABAergic neurons, while very low expression is detected in dopaminergic and noradrenergic neuronal populations (reviewed in *11*). Finally, recent data from our laboratory revealed that *Cdkl5* mRNA is distributed throughout neuronal districts even in spines, where local translation may participate in spine dynamics (*15*).

2.3 CDKL5 protein

CDKL5 is a member of the CMGC serine/threonine protein kinase group, which shares homologies with mitogen-activated kinases (MAPK) and cyclin-dependent kinases (CDK).

CDKL5 is characterized by a N-terminal serine/threonine catalytic domain (aa 13-297), which comprises an ATP-binding region (aa 13-43) and a protein kinase active site (aa 131-143) (reviewed in *11*). Within the catalytic domain is also present a Thr-X-Tyr (TEY) motif (aa 169-171) whose dual phosphorylation is reported to activate, among others, kinases of the MAPK family (*16*). CDKL5, as some other proteins of the CMGC group, can autophosphorylate its TEY motif. Despite CDKL5 is known to exist as a number of different isoforms, they all share the same catalytic domain, whereas differences are found in the C-terminus of the protein. An unusual long C-terminal tail, which plays an important role in regulating the subcellular localization, is unique for CDKL5. As a matter of fact, putative signals for nuclear import (NLS_1 aa 312-315; NLS_2 aa 784-789) and export (NES 836-845) have been recognized in the C-terminal tail (Image 1).

At the cellular level, CDKL5 can be detected in all NeuN-positive neurons, while it is expressed at very low levels in glia. As previously mentioned, CDKL5_1 is the most expressed isoform in brain and its functions seem to be regulated both through subcellular localization, synthesis, and degradation. In cortex, CDKL5 is equally distributed between nucleus and cytoplasm but studies performed in cultured hippocampal neurons revealed that specific stimuli can induce the translocation of CDKL5 from the nucleus to the cytoplasm through an active nuclear export mechanism mediated by the CRM1 receptor (*17*, *18*).

Proteasome-dependent degradation has been reported to be involved in modulating CDKL5 levels. Publications from our laboratory showed that sustained stimulation with both glutamate and KCl strongly reduce Cdkl5 levels in primary hippocampal cultures; this reduction, which occurs after a short-lasting induction of Cdkl5 protein synthesis, was prevented by the application of the proteasome-inhibitor MG132. It is worthwhile to note that MG132 treatment alone resulted in an increase of Cdkl5 levels, indicating that the proteasome constitutively regulates the turnover of the protein (*15*, *17*). Moreover, it has been shown that Cdkl5 interacts Mind bomb 1 (Mib1), an E3 ubiquitin ligase, that concurs in regulating neurite outgrowth in post-mitotic neurons, as well as long-term potentiation and synaptic plasticity in mice (*19–21*). Mib1 overexpression leads to a strong downregulation of CDKL5 in a dose dependent manner, suggesting that the Mib1 ligase activity is required for the proteasome-dependent induced change of CDKL5 abundance (*19*).

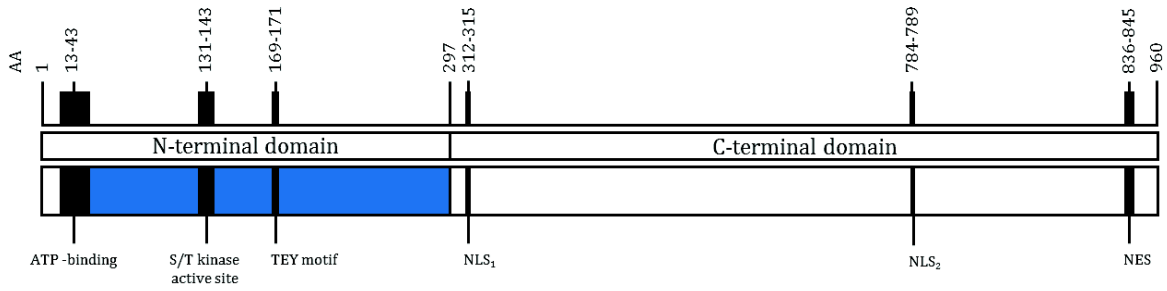

Image 1| Schematic representation of hCDKL5_1 with the functional domains and signatures indicated. NLS: nuclear localization signal; NES: nuclear export signal. Kinase domain is depicted in blue. Numbering refers to amino acid.

2.4 *CDKL5* pathological variants

To date, 245 different *CDKL5* variants have been described in literature (RettBASE: RettSyndrome.org Variation Database mecp2.chw.edu.au. Accession date: February, 2017) (*22*). Among these, 161 were classified as pathogenic or likely pathogenic variants, including missense and nonsense mutations, splice variants, exonic deletions, in-frame or frameshift mutations and multiple mutations (combinations of nonsense and missense mutations in the same patient) (Table 3). Moreover, Xp22 duplications involving *CDKL5* gene have been described (*23*).

Mutations	N. of entries	
	Pathogenic	Likely pathogenic
Missense	15	21
Nonsense	22	
Splicing variant	20	1
Exonic deletion	24	1
In-frame deletion or insertion		1
Frameshift deletion or insertion	53	
Multiple mutations	3	

Table 3| Summary of *CDKL5* pathogenic or likely pathogenic variants reported in RettBASE (*22*) (Accession date: February, 2017).

Notably, missense mutations localize mainly in the catalytic domain underscoring the importance of the kinase activity of CDKL5 for proper brain functions. On the contrary, truncating mutations can occur anywhere in the gene, resulting, if the transcript does not undergo nonsense-mediated decay, in CDKL5 derivatives of various lengths. Several studies have tried to elucidate the molecular effects of CDKL5 pathological mutations through the overexpression of CDKL5 mutants in non-neuronal cell lines (*18*, *24*, *25*). These studies revealed that missense mutations impact negatively on the catalytic activity of CDKL5, while C-terminally truncated derivatives prevalently localize in the nucleus. It is important to mention that the C-terminal tail also acts as a negative regulator of catalytic activity. Whether CDKL5 C-terminal mutants act as loss- or gain- of function proteins is still to be understood. Since CDKL5 exerts its roles both in the cytoplasm and in the nucleus, the absence of truncated derivatives from the cytoplasm might be involved in the pathological phenotypes. The limited number of patients still hampers drawing any genotype-phenotype correlation. Recently, Fehr and colleagues analysed the existence of a correlation in the largest number of CDKL5-confirmed cases (124 patients) harbouring different mutations (*26*). They found that those patients with late truncating mutations in the C-terminal domain (with a truncation after aa 781) had better communication skills and were more likely to be able to stand or walk independently than those predicted to have no functional protein. Clearly, larger studies are needed to better investigate the roles of different CDKL5 variants on

protein expression, function, and on the clinical phenotype. Finally, also the increased dosage of CDKL5 due to genomic duplication concurs in clinical manifestations, including difficulties in learning, autistic and hyperactive behaviour, developmental and speech delay, and macrocephaly. All these data suggest that unbalanced CDKL5 expression and activity can lead to perturbations of synaptic development and plasticity.

2.5 Roles of CDKL5 in synaptic function, morphology and plasticity

Growing pieces of evidence have accumulated supporting the hypothesis that CDKL5 is directly involved in neuronal functions and plasticity. Firstly, CDKL5 expression correlates, both *in vivo* and *in vitro*, with neuronal maturation and remains high in the adulthood (*18*), suggesting that the kinase might play a role not only in neuronal maturation but also in maintaining neuronal functions.

Interestingly, recent data from our laboratory demonstrated that CDKL5 levels respond promptly to neuronal activity and the kinetics of protein expression and decline are tightly regulated and change dramatically between different developmental stages (*15*). As a matter of fact, KCl-induced CDKL5 up-regulation is maintained for a longer time after stimulation in immature neurons, whereas at further stages of maturation the expression of the kinase return to basal levels, or even lower, within few minutes. Moreover, activation of local protein synthesis in dendrites and spines seems to be the main mechanism involved in the stimulus-dependent regulation of CDKL5 expression and rely, in mature neurons, on calcium influx through NMDA and AMPA receptor. Furthermore, NMDA receptor activation is mandatory for the subsequent PP1-dependent CDKL5 dephosphorylation and rapid degradation. CDKL5 thus behaves similarly to cAMP response element-binding protein (CREB), a transcription factor widely known to be implicated in synaptic plasticity, the expression and phosphorylation status of which rely on NMDA receptor activation (*27*).

The co-localization of CDKL5 with post-synaptic density protein 95 (PSD95) and SHANK, both *in vitro* and *in vivo*, and its juxtaposition to VGLUT, led Ricciardi and colleagues to relate CDKL5 to glutamatergic synapses (*28*). Synaptic targeting of CDKL5 seems to be regulated both by the presence of its mRNA that undergoes local translation upon stimuli, as mentioned above, and the direct interaction with synaptic proteins such as PSD95 and netrin-G1 ligand (NGL-1) (*28*, *29*). PSD95 is a post-synaptic scaffolding protein that regulates synaptic

accumulation of its binding partners. For instance, AMPA receptor targeting and stabilization at the post-synaptic membrane is mediated by PSD95 through the direct interaction with the AMPA receptor interacting protein stargazin. Similarly, CDKL5 synaptic targeting is promoted by its interaction with the palmitoylated form of PSD95 or by the formation of a complex involving PSD95 and NGL-1. NGL-1 is a regulator of synapse formation and homeostasis and its phosphorylation at serine 631, mediated by CDKL5, is necessary to ensure stable binding to PSD95. The synaptic targeting of CDKL5 suggests its involvement in molecular pathways that regulate synaptic maturation and function. As a matter of fact, RNA interference analyses showed that loss of CDKL5 affects spine morphology and excitatory synaptic functions. Consistent data showed that CDKL5-knock down, both *in vitro* and *in vivo*, results in phenotypical *filopodia*-like immature spines, reduced excitatory synaptic puncta and decreased amplitude and frequency of miniature excitatory post-synaptic currents (mEPSCs) (*28*, *29*).

To study CDKL5 loss-of-function *in vivo*, two independent laboratories have generated *Cdkl5*-null mouse models that mirror some clinical aspects of the human disease (*30*, *31*). In particular, the Wang model shows motor defects, reduced anxiety, decreased sociability, altered EEG activity, and impaired learning and memory, which are core features of CDKL5-related disorder (*30*). These ethological phenotypes mimic the impaired motor skills, reduced social interaction and intellectual disability observed in CDKL5 patients. Interestingly, neither of the two mouse models shows the characteristic onset of spontaneous seizures even though Amendola and colleagues demonstrated an abnormal EEG response upon treatment with the pro-convulsant kainic acid (*31*). Importantly, the absence of an epileptic neuronal network suggests that the behavioural and electrophysiological defects observed in these mice are primary consequences of CDKL5 loss-of-function.

Notably, serine/threonine kinome studies on *Cdkl5*-null brains revealed alterations of many signal transduction pathways, including that of AKT-mTOR, which has been implicated in the etiology of autism spectrum disorders and RTT. In addition to the AKT-mTOR pathway, loss of CDKL5 alters the phosphorylation profile of other kinases involved in synaptic plasticity including PKA, PKC and PKD (*30*). These alterations may be indirect effects of CDKL5-loss, but suggest once more that CDKL5 is crucial for the coordination of multiple signalling pathways involved in synaptic plasticity.

Similarly to CDKL5 RNA-interference experiments, *Cdkl5*-null brains show a decrease in excitatory synaptic puncta in the CA1 field of hippocampus as result of a lower spine density. Moreover, immunohistochemical characterization of spine shape revealed a higher percentage of immature spines (filopodia, thin- and stubby-shaped) in *Cdkl5*$^{-/y}$ neurons compared to wild type neurons (*32*). To dissect out the role of CDKL5 in spine formation, stability and elimination during development, Della Sala and colleagues have taken advantage of cranial window implantation overlying the somatosensory cortex followed by two-photon imaging at different time points (*33*). During early development, *Cdkl5*-null brains display significant reduction of spine density and PSD95-positive puncta when compared to wild type littermates. Conversely, the density of filopodia was similar between the two genotypes, suggesting that CDKL5 is not involved in the formation of new spines but rather in the stabilization of mature mushroom-shaped spines. As matter of fact, the decreased spine density in *Cdkl5*$^{-/y}$ mice can be attributed to lower spine survival rate. As result, the authors showed a dramatic decrease in mEPSCs frequency and long-term potentiation impairment in *Cdkl5*-null cortical slices.

Altogether, these data suggest that CDKL5 can be considered as a new plasticity molecule that seems to be crucial for the regulation of spine dynamics and for learning and memory.

2.6 AMPA receptor structure and subunit composition

More than forty years have passed since Bliss and Lømo used rabbit hippocampi to demonstrate for the first time that a stimulus could cause an increase in synaptic strength that was long lasting, named long-term potentiation (LTP)(*34*). The discovery of LTP laid the foundation for a remarkable number of studies aimed to understand how memories are stored in synapses and whether changes in these structures underlie the ability to learn new behaviours.

A particular class of glutamatergic receptors, the cation-permeable ionotropic alpha-amino-3-hydroxy-5-methyl-4-isoxazole propionic acid (AMPA) receptors (AMPARs), mediate most fast excitatory synaptic transmission in the central nervous system and are one of the key determinants of synaptic strength and plasticity (*35*). AMPARs are expressed throughout the brain and are composed by four subunits (GluA1-GluA4), also known as GluR1-GluR4, which are encoded by the genes *GRIA1-GRIA4*, and are assembled as dimers-of-dimers to form

homo- or hetero-tetramers (Image 2-A) (*36*). Most AMPARs in adult hippocampus and cortex consist of GluA1 plus GluA2 or GluA2 plus GluA3 subunits, but since GluA3 is expressed at relatively low levels, GluA2 is prevalently found associated with GluA1 (*37*, *38*). Contrariwise, GluA4 is tightly developmentally regulated and is barely expressed in the adult brain where it is a key determinant of AMPAR-mediated transmission in parvalbumin-containing inhibitory interneurons (*39*–*41*).

All AMPA receptor subunits comprise an extracellular amino-terminal domain (ATD or NTD), a ligand binding domain (LBD) (S1 and S2), three membrane-spanning domains (M1, M2 and M3), one cytoplasmic re-entrant loop (P), and an intracellular carboxy-terminal domain (CTD) (Image 1-B) (*36*, *42*, *43*). The extracellular and transmembrane domains are highly homologous whereas the main differences can be found in the intracellular cytoplasmic tails. GluA1 and GluA4 have long cytoplasmic tails, whereas GluA2 and GluA3 have short C-terminal tails. Alternative splicing can generate different splice forms of GluA2 and GluA4, named GluA2L and GluA4S, characterized by a longer (L) or shorter (S) tail (*44*, *45*). Moreover, alternative splicing also generates the *flop* (shorter) and *flip* (longer) variants of AMPARs, encoded by exon 14 and 15, respectively, that differ by a 38-amino-acids insertion in the LBD. While the expression of the *flop* variants increases during development, the expression of the *flip* variant remains prominent and unchanged not only in the post-natal development but also during gestation (*46*, *47*).

2.7 Biophysical and molecular properties of AMPA receptors

The release of the neurotransmitter glutamate from the presynaptic density activates post-synaptic ion channels including AMPARs, N-methyl D-aspartate (NMDA) and kainate (KA) receptors. Once activated, the glutamate-gated ion channels flux sodium (Na^+) and in some cases also calcium (Ca^{2+}). NMDARs are uniformly Ca^{2+}-permeable (*48*), whereas AMPARs and KA receptors exist in both Ca^{2+}-permeable and -impermeable forms depending on the precise subunit composition and RNA editing. In the adult brain, almost all GluA2 (~99%) have a positively charged arginine (R) in the M2 channel-forming segment at position 607 (Q/R site) (Image 1-B), while other AMPAR subunits have glutamine (Q) at this position (*49*). This difference is caused by RNA-editing in which the site-selective deamination of adenosine (A) in the critical C<u>A</u>G codon in the pre-mRNA to an inosine (I) creates a C<u>I</u>G codon (*50*). Since

the ribosomes read the inosine as a guanosine (G), the edited codon alters the coding potential and an R is inserted in place of Q. The resulting edited GluA2(R) prevents Ca^{2+} influx when it is incorporated in the AMPAR. Conversely, AMPARs containing unedited GluA2(Q) are highly permeable to Ca^{2+}. When glutamine is present, a negative electrostatic potential is formed with the N-terminus of the M2 loop and cations are thus attracted. However, the replacement of the neutral glutamine with a large positively charged arginine residue neutralizes the negative electrostatic potential and thus prevents the diffusion of divalent cations through the pore (*51*). Deamination is performed by ADAR2, a double-stranded-RNA-specific adenosine deaminase and the principal RNA-editing enzyme in mammals (*50*). Unedited GluA2(Q) exists during embryogenesis where it seems to have an important role in directing human neural progenitor cell differentiation to neurons (*52*).

The precise number and subunit composition of AMPARs determine the efficiency and dynamics of AMPAR-mediated synaptic signalling, in particular, different subunit composition confer distinct biophysical and molecular properties to AMPARs. For example, GluA2-containing receptors display a linear current-voltage relationship and are impermeable to Ca^{2+} (*53*). In contrast GluA2-lacking receptors display double rectification, have higher single-channel conductance and are Ca^{2+}-permeable (*54*). Moreover, *flip*/*flop* variants influence the response to AMPAR potentiators, with *flop* versions being less responsive and de-sensitizing more rapidly to glutamate than *flip* variants (*46*, *55*, *56*).

2.8 AMPA receptor-interacting proteins

AMPAR trafficking, synaptic targeting and recycling relies on interactions with a large number of proteins comprising those that interact alternatively with the NTDs and CTDs.

2.8.1 NTD-interacting proteins

To date only two proteins have been described to interact with the NTD of all four AMPAR subunits: neuronal pentraxin 1 (NP1) and neuronal immediate early gene neuronal activity-regulated pentraxin (NARP). While NP1 is important in homomeric GluR4 clustering during synaptogenesis, NARP is fundamental for GluA1-, GluA2- and GluA3-AMPAR clustering and stabilization at excitatory synapses (*57*, *58*). GluA2 NTD has also a specific interaction site for N-cadherin, an important transmembrane protein, which concurs in pre- to post-synaptic

adhesion. GluA2 NTD is required non only for morphological spine changes in length and width but also for spine number, suggesting that GluA2-containing AMPAR may stimulate spine formation and development through structural interaction at the synaptic junction (*59*, *60*).

2.8.2 CTD-interacting proteins

PDZ (Post-synaptic density 95/Discs large/Zona occludens 1) domain-mediated protein interactions have been shown to play important roles in the regulation of glutamate receptor function at excitatory synapses. In the cytoplasmic compartment, several PDZ-containing molecules interact with the CTD of AMPARs (Image 1-C). SAP97, a member of the membrane-associated guanylate kinase (MAGUK) family, binds simultaneously the C-terminus of GluA1 through its PDZ domain and AKAP79 (protein kinase A anchoring molecules), which may promote GluA1 phosphorylation required for LTP (*61–63*). Moreover, SAP97 has also been described to act in the early secretory pathway to facilitate AMPAR maturation (*64*). GluA2 and GluA3 share a C-terminal sequence (SVKI), which interacts with the PDZ-containing molecules GRIP1, GRIP2 (ABP), and PICK1. To date, several studies have shed light on the important roles of GRIP1/2 and PICK1 in AMPAR trafficking and synaptic plasticity (*65–67*). Other non-PDZ-containing molecules are able to interact with AMPARs in a subunit-specific manner (Image 1-C). Among these, 4.1N protein, the neuronal isoform of red blood cell actin cytoskeleton associated protein 4.1R, appears to be involved in AMPAR stabilization at the cell surface by the interaction with GluA1 (*68*). On the other hand, the interaction between the ATPase NSF and GluA2 is required for the insertion and subsequent stabilization of GluA2-containing AMPARs in the membrane (*69*), while AP2 interaction, in a region overlapping the NSF binding site, is involved in clathrin-mediated endocytosis during LTD (*70*).

Among the large number of CTD-interacting protein there is another group of molecules named *AMPA auxiliary proteins,* which are important for AMPAR targeting and stabilization at the post-synaptic membrane. This group of molecules includes the transmembrane AMPA regulatory proteins (TARPs)(*71–73*). TARPs are classified into six isoforms - type 1a (γ-2/stargazin and γ-3), type 1b (γ-4 and γ-8) and type 2 (γ-5 and γ-2) - according to how they control AMPAR trafficking and channel properties. Owing to incompatible PDZ ligands,

AMPARs do not bind directly to the synaptic scaffold protein PSD95. Instead, TARPs bind to PSD95 like MAGUK proteins to stabilize the AMPARs at the post-synaptic membrane. Moreover, TARPs differentially modulate channel properties not only by selectively stabilizing specific AMPAR channel conformations, but also by altering the structure of the AMPAR pore (*74*).

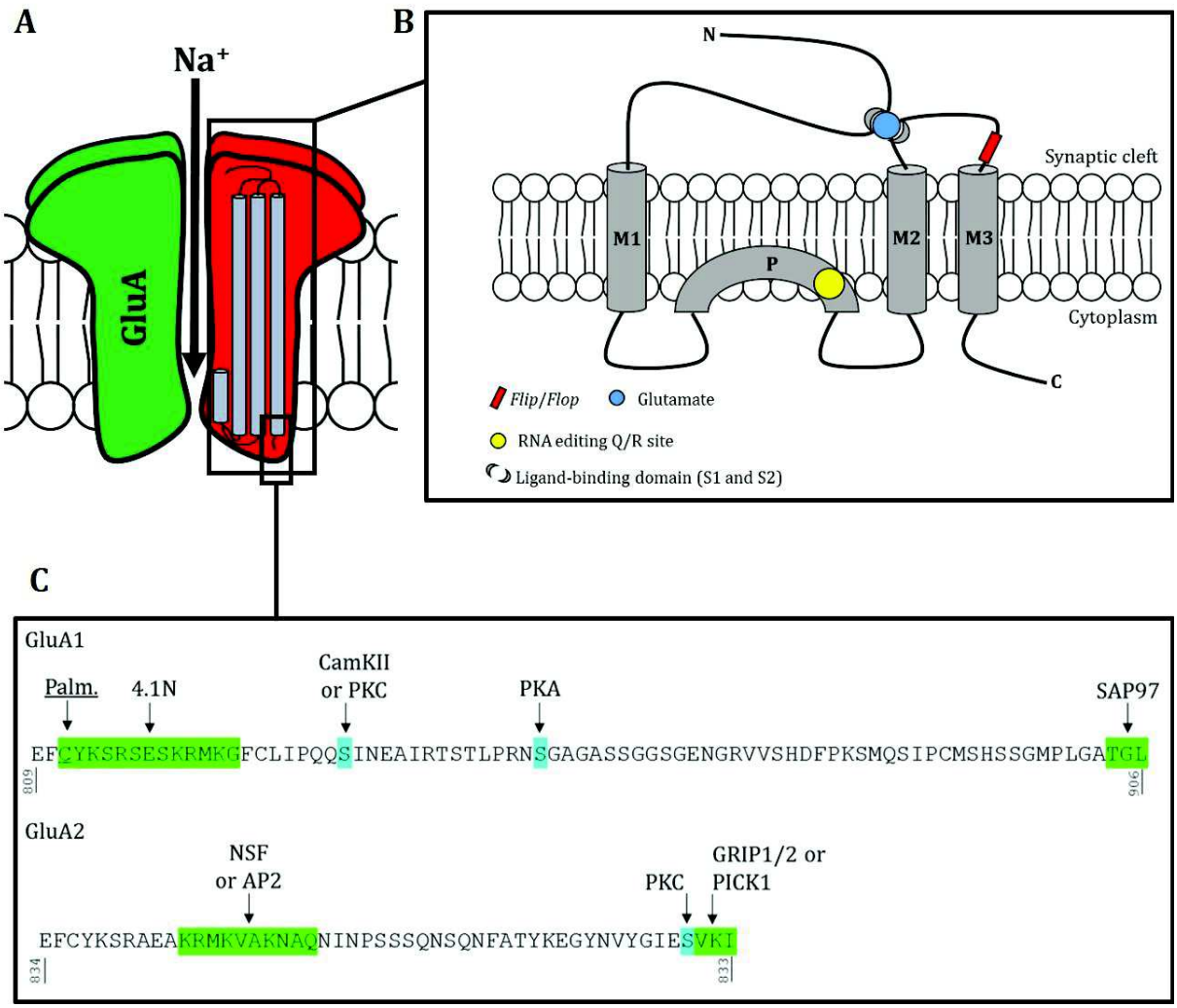

Image 2| (A) Schematic illustration of AMPAR tetramer in membrane. Tetrameric AMPARs are assembled from two dimers of distinct subunit composition. (B) Schematic illustration of the GluA subunit structure. Each subunit has an extracellular amino-terminal domain (ATD or NTD), three full trans-membrane domains (M1, M2 and M3), an intracellular re-entrant loop, which is the site of Q/R editing in GluA2, and an intracellular carboxy-terminal domain (CTD). Each GluA subunit is composed of a large extracellular ligand-binding core (segments S1 and S2) that serves as binding site for glutamate. In red is depicted the site of the alternative splice

flip and *flop* variants that control gating kinetics. (C) Sequences of the intracellular CTDs of the predominant isoforms of human GluA1 and GluA2 indicating protein interaction sites (in green), phosphorylation sites (in blu) and a palmitoylation site (underlined).

2.9 AMPA receptor biosynthesis and trafficking

Similarly to most multimeric trans-membrane proteins, AMPARs are first assembled in the endoplasmic reticulum (ER). The initial dimerization is a heterodimer assembly, which preferentially incorporates GluA2 subunits in the nascent receptor; however, dimerization of GluA2-lacking AMPARs is also possible under appropriate physiological and pathological conditions (*75*–*77*). This initial process involves the interaction between the NTDs of two subunits, followed by a second dimerization step that is mediated by associations at the LBD (*78*). Against this background, most assembled AMPAR tetramers contain GluA2 subunits that profoundly influence receptor trafficking, slowing ER export of new receptors. AMPARs that contain both GluA1 and GluA2 subunits exit rapidly from the ER overriding the ER retention of GluA2 whereas GluA2/GluA3 homo/heteromers transit much slower (*49*, *79*). It is important to recall that the GluA2 subunit is strongly regulated by Q/R editing and the arginine arising from this event of maturation influences not only channel properties but also receptor trafficking. Unedited GluA2(Q), whenever present, traffics rapidly through the ER similarly to GluA1. The Q/R editing results in a stable pool of GluA2 subunits that exit the ER in a heteromeric complex in a more regulated manner (*49*).

As previously described, AMPARs can interact with many proteins through their CTD, and some of these proteins may regulate ER retention or exit. Among these proteins, PICK1 is not only involved in AMPAR endocytosis and/or recycling but seems also to be necessary for the exit of GluR2 from the ER while SAP97 seems to have the same function towards GluR1 (*80*, *81*). AMPAR biosynthesis and the secretory pathway involve not only the somatic Golgi apparatus but also the dendritic Golgi compartments representing the outposts of post-translational modifications of proteins that are translated locally (*82*). Within the Golgi, AMPAR subunits and AMPAR-associated proteins undergo lipid modifications and, between these, palmitoylation plays important roles in synaptic function (*83*, *84*). Palmitoylation is a reversible process regulated by palmitoyl acyl transferases that attach covalently palmitate moieties via a thioester bond to cytosolic cysteine residues. PSD95 and GRIP1/GRIP2

pamitoylation positively regulate AMPAR accumulation at synapses and AMPAR trafficking toward the membrane (*84*–*86*). AMPA receptor palmitoylation can occur on a cysteine near the Q/R editing site and in the CTD (*87*). Palmitoylation of AMPAR CTD negatively regulate the interaction with 4.1N resulting in a minor surface expression and increased internalization (*68*).

The architecture of neurons, which are characterized by high polarization and an elaborate structure, poses the problem for the trafficking of membrane proteins, including AMPARs, that is further exacerbated by the very long distances between the soma and their final locations. AMPARs are trafficked along dendrites in a microtubule-dependent manner; this transport is an active process involving motor proteins such as kinesin and dynein (*88*). The PDZ-containing proteins GRIP1/GRIP2 interact directly with the heavy chain of kinesin (KIF5) together with the CTD of GluA2/GluA3 subunits (*89*). Moreover, the KIF1-interacting protein Liprin-α can bind GRIP1/2-GluR2 complex suggesting that GRIP1/GRIP2 proteins serve as an adaptor to link AMPAR to kinesins and promote dendritic transport (*90*). In addition, neurons have evolved specific pathways to transport mRNA into dendrites, where subsequent local translation can occur. Most mRNAs transported into dendrites are those encoding proteins involved in synaptic transmission, such as Arc, calcium/calmodulin protein kinase II (CamKII), brain-derived neural factor (BDNF) and some AMPAR subunit mRNAs, suggesting that local synthesis of AMPAR subunits regulates local receptor abundance and composition (*91*). Notably, the group of mRNAs that undergo stimulus-dependent local translation has recently been found to comprise that of *CDKL5* (*15*).

2.10 AMPAR trafficking in LTP and LTD

Hebbian plasticity is a mechanism that gives rise to long-lasting changes in synaptic strength, including LTP and LTD. These opposite phenomena both start with presynaptic terminal depolarization and subsequent activation of NMDA receptors, which allows Ca^{2+} entrance at the post-synaptic site. A strong but brief increase in Ca^{2+} concentration gives rise to LTP, whereas a low but continuous Ca^{2+} influx promotes LTD (*92*, *93*). Intracellular Ca^{2+} acts on several signalling pathways including those involving kinases, such as, calcium/calmodulin protein kinase I and II (CamKI/II), cAMP-dependent PKA and PKC, but also phosphatases, such as protein phosphatase 1 (PP1), 2A (PP2A) and 2B (PP2B). Both kinases and

phosphatases regulate AMPAR trafficking to and from the post-synaptic membrane, influence AMPAR composition over longer term, affect pre-existing post-translational modifications influencing channel permeability and, finally, regulate the interactions between AMPARs and AMPAR-interacting proteins (*44*).

LTP is characterized by the long-lasting potentiation of AMPAR-mediated excitatory post-synaptic currents (EPSCs). An emerging consensus is that the transient membrane expression of calcium-permeable AMPAR (CP-AMPAR), those arising from either the lack of GluR2 subunits or from the presence of unedited of GluA2, contributes to the induction, but not the maintenance, of LTP (*94*–*96*). During LTP induction, CP-AMPARs are recruited to synapses from perisynaptic sites to contribute to Ca^{2+} entry followed by NMDAR activation. This results in stimulation of CamKII, PKA and PKC that catalyze GluA1 phosphorylation (Image 1-C). The phosphorylation state of GluA1 is critical for AMPAR recruitment to post-synaptic sites. Specifically, four serine residues can be phosphorylated during LTP (Ser831 by CAMKII and PKC; Ser845 PKA; Ser816 and Ser818 by PKC). These phosphorylation events not only enhance the binding of GluA1 to 4.1N, which stabilizes the receptor at the post-synaptic density, but also increase the conductance and opening probability of the channel (reviewed in *64*). The Ca^{2+} that is gated from CP-AMPARs contribute the recruitment of CI-AMPARs, containing edited GluA2 subunits. Until CP-AMPARs are replaced with CI receptors, LTP remains unstable and easily reversible. It should be noted, however, that the involvement of CP-AMPARs in LTP is not universally accepted (*98*, *99*); therefore the roles, the timing and extent of CP-AMPAR/CI-AMPAR incorporation in the post-synaptic membrane during LTP still remain an open field of research.

Contrariwise, LTD is characterized by the loss of synaptic AMPARs evoked by NMDARs or metabotropic glutamate receptor activation (*92*). Upon NMDA stimulation, GluA2-containing AMPARs diffuse laterally to extrasynaptic sites where they are internalized in a clathrin-dependant manner via the clathrin adaptor AP2, which promotes the assembly of a clathrin coat (*70*). AP2 binds a region overlapping the NSF interaction site within GluA2 and during LTD the affinity of GluA2 for NSF is lost allowing the binding of AP2, which promotes AMPAR internalization (*70*). Several other GluA2-interacting proteins have been shown to regulate AMPAR trafficking in LTD; between these, GRIP1/2 and PICK1 are the best characterized (*65*, *100*). While GRIP1/2 promote GluA2 surface stabilization and recycling after internalization,

PICK1 promotes GluA2 internalization and retention in intracellular compartments during LTD. The affinity of GRIP1/2 and PICK1 for GluA2 is regulated by the phosphorylation status of serine 880 within the AMPAR subunit (Image 1-C). During LTD the activation of PKC triggers ser880 phosphorylation switching the affinity of GluA2 from GRIP1/2 to PICK1 thus promoting receptor internalization (*101–104*).

2.11 AMPAR subunits and disease

The fine tuning of AMPAR synaptic expression as well as the mechanisms that control their trafficking and activity are necessary for proper brain function. Indeed, most neurological and neurodegenerative disorders can be linked to AMPAR deregulation that underlies synaptic malfunctions. For example, variants of *GluA3*, which cause loss of GluA3 function due to gene deletion, reduced protein expression, or loss of channel current have been associated with moderate mental retardation (*105*). Moreover, reduced synaptic AMPARs is one of the earliest biological manifestations of dementia in Alzheimer disease (AD); indeed, soluble amyloid-β oligomers disrupts GluA2 trafficking resulting in intracellular retaining of the receptor (*106*). Furthermore, the synaptic loss of GluA2-containing AMPARs in AD results in the enhancement of surface-expressed CP-AMPARs and consequent excitotoxicity (*107*).

The switch from CI-AMPARs to CP-AMPARs owing to the loss of GluA2-containing receptors is implicated in the pathology of many other diseases. In particular, CI- to CP-AMPAR switch is the causal factor of neuronal death in ischemia and traumatic brain injury (*108*). Moreover, neurons subjected to epileptic seizures markedly down-regulate GluA2 mRNA and subunit expression (*109*).

Recently, alterations of the AMPA-receptor mediated neurotransmission have been linked with autism spectrum disorders. For instance, loss of the autism-related genes, such as Rab39b and Mecp2, results in a preponderant expression of CP-AMPARs at the post-synaptic membrane (*110*, *111*).

These observations suggest that aberrant GluA2 incorporation in AMPARs is strongly implicated in neuronal disease and highlight the importance of maintaining the balanced expression CP- and CI-AMPARs for neuronal functionality. However, much remains to be investigated to fully understand how the pathways involved in AMPAR dynamics are modulated, possibly serving as basis for the rationale design of therapeutic interventions.

3. RESULTS

3.1 CDKL5 knock-down differentially affects the expression level of AMPA receptor subunits

As mentioned above, several pieces of evidence suggest that loss of CDKL5 negatively impacts on spine number and morphology, as well as on LTP and learning and memory. To date, the molecular mechanisms that underlie these phenomena have not been completely understood. Therefore, we decided to focus our attention on AMPARs, which play important roles in spine dynamics and plasticity-related mechanisms. To address this point, mouse primary hippocampal neurons were silenced for Cdkl5 at *days in vitro* 0 (DIV) with lentiviral particles carrying either one of two different shRNAs (sh#1; sh#2), or shLacZ as control. AMPAR subunit expression was evaluated after 16-18DIV by Western blotting analysis using the signal of neuron-specific Class III β-tubulin (Tuj1) as internal standard. The analyses were performed on mature neurons, as already demonstrated by our group by the appearance of functional synapses between neurons characterized by GluA2-positive dendritic punctae juxtaposed to synapsin 1-positive presynaptic dots from 14 days in vitro (*15*). Lentiviral infection with sh#1 and sh#2 efficiently silenced Cdkl5 expression (sh#1: 0.364±0,071, $p<0.001$; sh#2: 0.212±0.051, $p<0.001$) **(Fig. 1A-C)**. Importantly, Cdkl5-silcencing significantly reduced AMPAR GluA2 subunit expression with both Cdkl5 shRNAs compared to the control (sh#1: 0.544±0.087, $p<0.001$; sh#2: 0.514±0.045; $p<0.001$), whereas expression of the GluA1 subunit was unaltered (sh#1: 0.89±0.124; sh#2: 0.987±0.092; $p=0.652$) **(Fig. 1B-C)**.

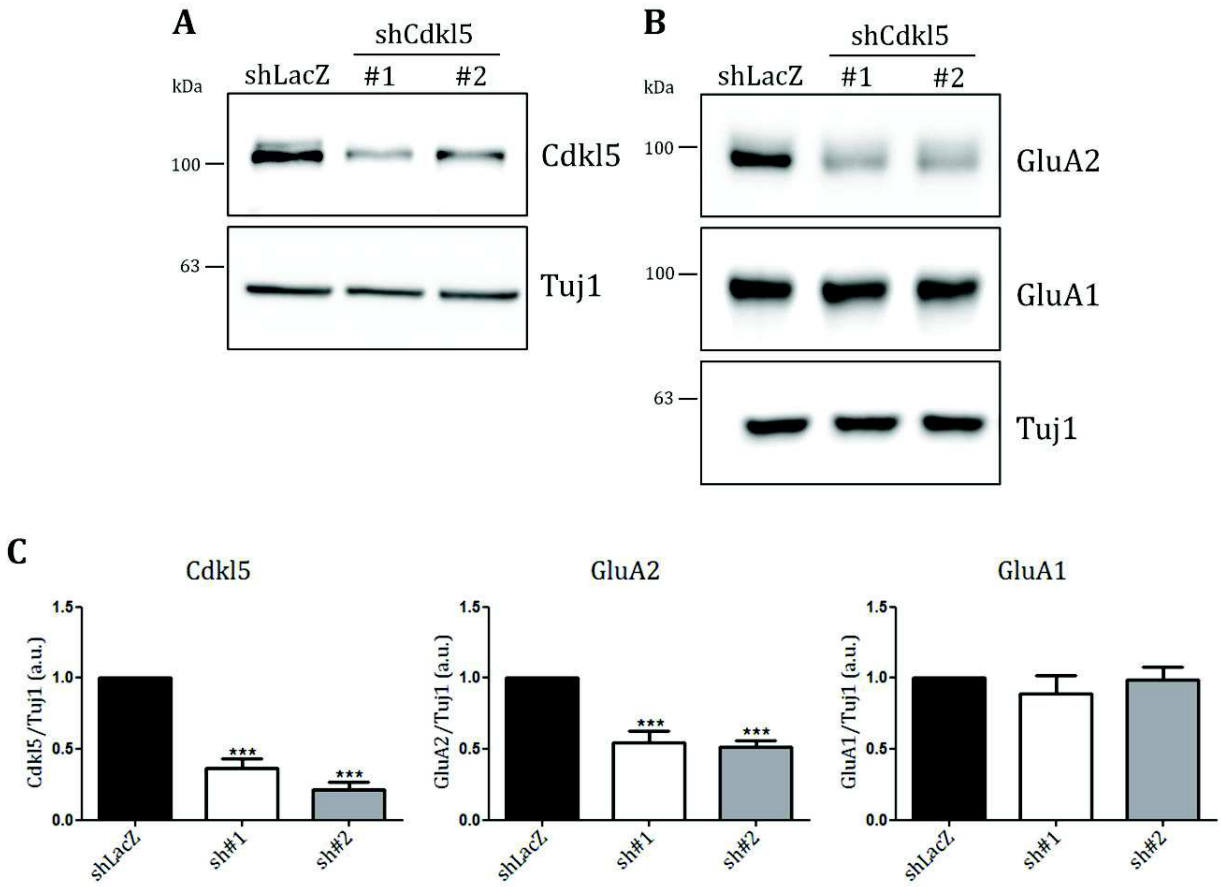

Fig. 1| CDKL5 knock-down differentially affects the expression level of AMPA receptor subunits. (A) Representative WB showing silencing of Cdkl5 expression in primary hippocampal neurons with two different shRNAs (#1 and #2) or, as control, shLacZ. Neurons were silenced at DIV0 and harvested at DIV16-18. The WB shows also GluA1 and GluA2 levels. Tuj1 was used as loading control. **(B)** Densitometric quantification of data shown in A. Analysis of n>7 independent experiments. Statistical analysis: One-way ANOVA followed by Dunnett's multiple comparison test; shCdkl5 vs shLacZ: ***p<0.001.

3.2 Altered expression of GluA2 subunit in Cdkl5-silenced neurons rely on post-transcriptional mechanisms

To test if AMPAR GluA2 subunit downregulation is due to altered gene transcription and mRNA abundance, primary hippocampal neurons silenced for Cdkl5 as above, were harvested at DIV16 and processed for mRNA extraction. As expected, RT-qPCR analysis revealed that *Cdkl5* mRNA levels were dramatically reduced after silencing compared to control (sh#1: 0.395±0.126, $p<0.01$; sh#2: 0.192±0.010, $p<0.001$), whereas *GluA2* mRNA levels were not affected (sh#1: 1.173±0.077; sh#2: 0.930±0.207; $p=0.472$) **(Fig. 2)**. These data revealed that Cdkl5-silencing does not alter *GluA2* gene expression, thus suggesting that reduced GluA2 protein levels rely on a post-transcriptional mechanism.

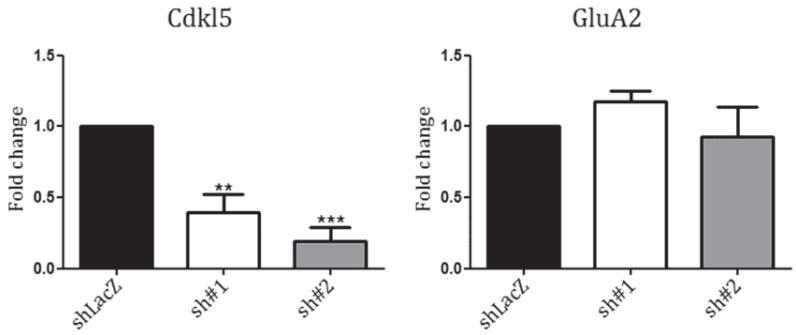

Fig. 2| *GluA2* mRNA levels are maintained in Cdkl5-silenced neurons. Quantification of *Cdkl5* and *GluA2* mRNA expression in primary hippocampal neurons silenced for Cdkl5 (sh#1 and sh#2) or, as control, LacZ. Neurons were silenced at DIV0 and harvested for mRNA extraction at DIV16. *Cdkl5* and *GluA2* mRNA levels were determined by RT-qPCR using the expression of *Gapdh* as internal standard. Analysis of n>4 independent experiments. Statistical analysis: One-way ANOVA followed by Dunnett's multiple comparison test; shCdkl5 vs shLacZ: **p<0.01; ***p<0.001.

3.3 Cdkl5 knock-down results in increased GluA2 phosphorylation at Serine 880

To understand the mechanism(s) underlying the post-transcriptional down-regulation of GluA2 levels in primary hippocampal neurons silenced for Cdkl5, we considered the phosphorylation levels of GluA2 Serine 880 (GluA2^{pS880}). As previously noted, S880 phosphorylation is a key post-translational modification involved in GluA2 internalization and subsequent lysosomal degradation during LTD. GluA2^{pS880} was thus evaluated after 16-18 *days in vitro* by Western blotting analysis as the ratio between phosphorylated and total GluA2 levels. Cdkl5 knock-down resulted in increased GluA2 phosphorylation when compared to the control sample (sh#1: 2.260±0.198, $p<0.001$; sh#2: 2.259±0.184, $p<0.001$) **(Fig.3 A-B)**.

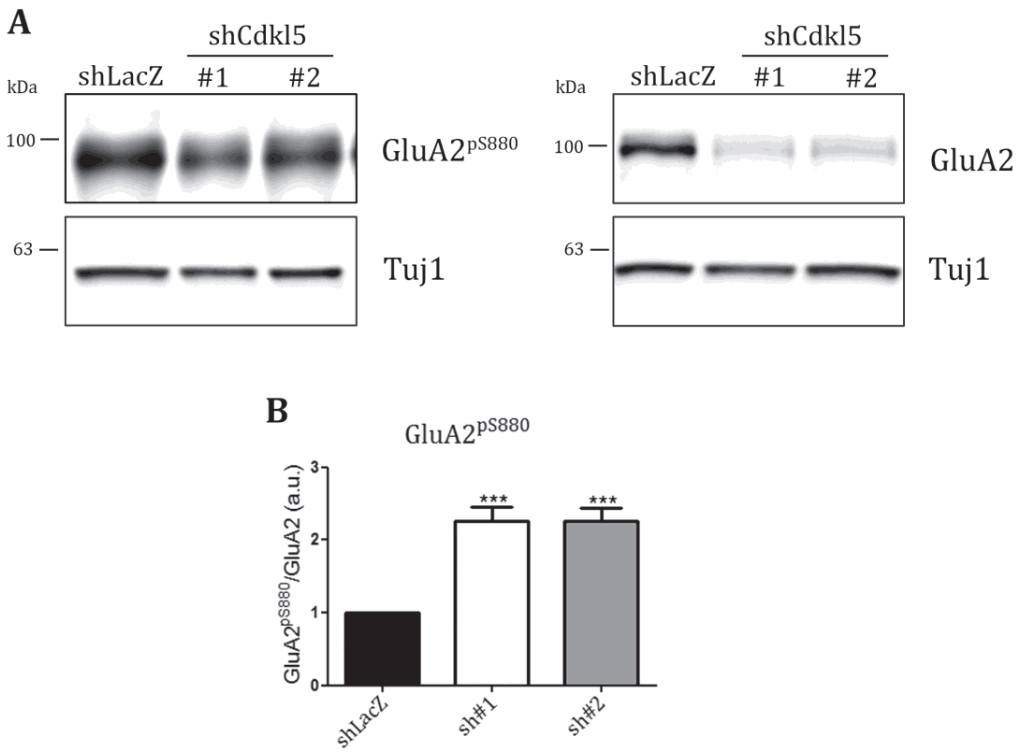

Fig. 3| Cdkl5 knock-down results in increased GluA2 phosphorylation at Serine 880. (A) WB showing GluA2 phosphorylation at Serine 880 (S880) and its total isoform in primary hippocampal neurons silenced for Cdkl5 with two different shRNAs (#1 and #2) or, as control, shLacZ. Neurons were silenced at DIV0 and harvested for WB analysis at DIV16-18. TUJ1 was used as loading control. **(B)** Densitometric quantification of data shown in A. GluA2^{pS880} was evaluated as the ratio between the phospho-protein and its total isoform. Analysis of n>5 independent experiments. Statistical analysis: One-way ANOVA followed by Dunnett's multiple comparison test; shCdkl5 vs shLacZ: ***$p<0.001$.

3.4 Cdkl5-silencing drives internalized GluA2-containing AMPARs to lysosomal degradation

To understand if the post-translational down-regulation of GluA2 could be explained by increased lysosomal degradation, we analyzed the co-localization between internalized GluA2-containing AMPARs and the lysosomal marker LAMP-1 by using the fluorescence-based antibody feeding assay. Firstly, silenced primary hippocampal neurons at DIV17 were *live* incubated with an antibody recognizing an extracellular epitope of GluA2 **(Fig. 4-A)**, then the cultures were stimulated for 2 min with AMPA (100 μM, in the presence of 50 μM of the NMDA receptor antagonist APV) to induce the internalization of surface-exposed GluA2-antibody complexes. To detect only the intracellular immuno-complexes, extracellular-bound antibodies were stripped away before fixation and staining for LAMP-1. Immunofluorescence analyses revealed a significant increase in the number of GluA2 punctae in Cdkl5-silenced neurons that mainly co-localized with LAMP-1 positive dots. In line with the hyper-phosphorylation at Serine 880 these data, even if still preliminary, might indicate that an increased amount of internalized GluA2 is directed towards lysosomal degradation in the absence of CDKL5 **(Fig. 4-B)**.

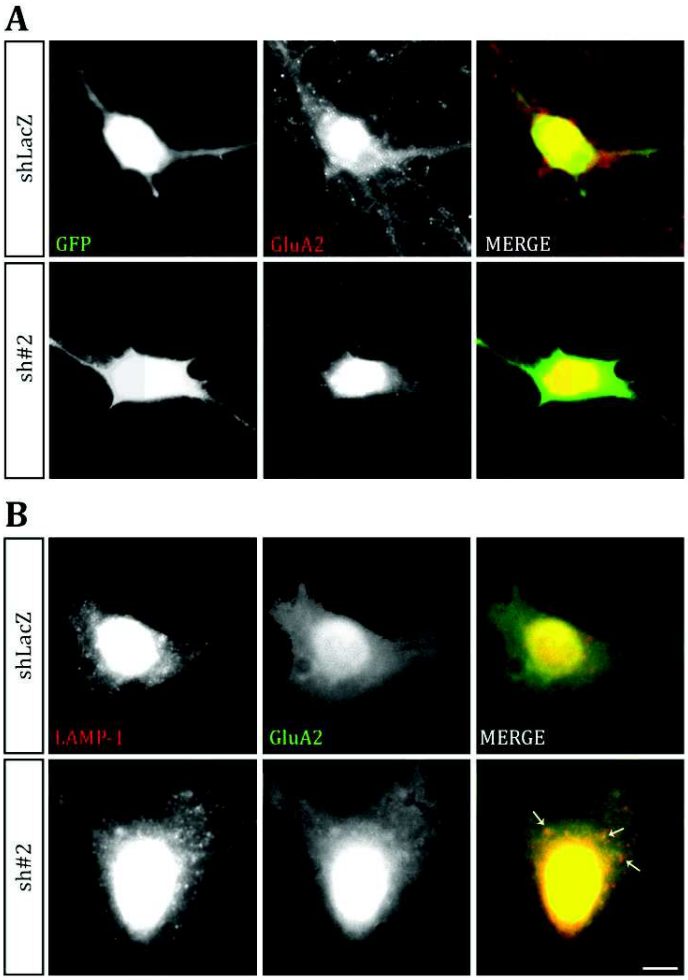

Fig. 4| Internalized GluA2 co-localizes with the lysosomal marker LAMP-1 in Cdkl5-silcenced neurons. **(A)** Representative images of surface GluA2 (red) in the soma of primary hippocampal neurons at DIV17, silenced for Cdkl5 (sh#2) or shLacZ, after live incubation with an antibody against an extracellular epitope of GluA2. **(B)** Representative images of internalized GluA2 (green) and lysosomal marker LAMP-1 (red) (pseudo-colors) in the soma of primary hippocampal neurons silenced for Cdkl5 after live incubation with GluA2 antibody followed by stimulation for 2 min with 100 μM AMPA and 30 min of recovery. Arrows indicate co-localization between internalized GluA2 and LAMP-1. Scale bar 5 μm. 16 neurons were analyzed in a single experiment.

3.5 Cdkl5 knock-out neurons and adult hippocampus recapitulate the biochemical alterations of AMPA receptor observed in Cdkl5-silenced cultures

The above data show that the abrupt ablation of CDKL5 interferes with AMPAR expression. To understand whether the same defect can be observed also upon the complete absence of CDKL5 during mouse brain development, we assayed GluA2 expression and Serine 880 phosphorylation in primary hippocampal neurons prepared from *Cdkl5*-null/*wild type* pups. Neurons were prepared at *post-natal day 0* and harvested at DIV16 for Western blotting analysis. Preliminary data indicated that loss of Cdkl5 impaired GluA2-subunit expression (0.69), whereas GluA1-subunit expression was less affected (0.91). Moreover, *Cdkl5*-null cultures showed increased GluA2 phosphorylation at Serine 880 (1.55) **(Fig.5 A-B)**. These results, albeit preliminary, suggest that the complete loss of Cdkl5 causes altered levels of AMPA receptor subunits; moreover, they validate the data obtained with Cdkl5-silenced cultures, demonstrating that the observed effects are specific for CDKL5. In line with the data obtained from both *Cdkl5*-null and -silenced cultures, adult *Cdkl5*-null hippocampi showed a significant reduction of GluA2-subunit expression (KO: 0.598±0.110 vs WT: 1.300±0.228, p=0.016), whereas GluA1 levels did not change significantly (KO: 2.180±0.408 vs WT: 1.254±0.294, p=0.111), suggesting that Cdkl5-related AMPAR defects are present also *in vivo* **(Fig. 5 C-D)**.

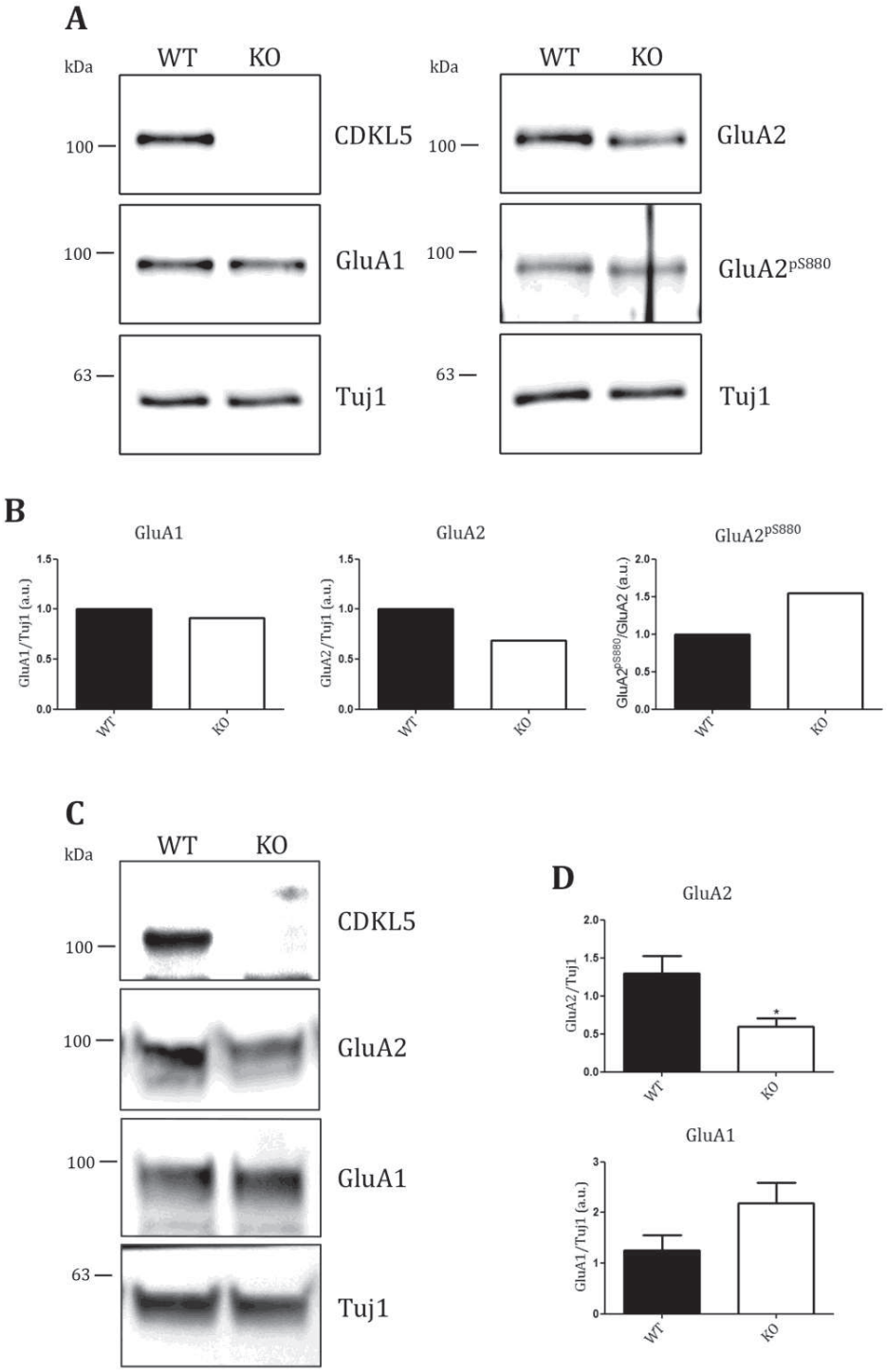

Fig. 5| AMPAR subunit defects are present in *Cdkl5*-null neurons and adult hippocampus. (A) WB showing GluA1-GluA2 expression levels of WT and *Cdkl5*-null primary hippocampal cultures harvested at DIV16. The WB also shows GluA2 phosphorylation at Serine 880 (S880) and its total isoform. Tuj1 was used as loading control. **(B)** Densitometric quantification of data shown in A. GluA2^{pS880} was evaluated as the ratio between the phospho-protein and its total isoform. (n=1). **(C)** WB showing GluA1-GluA2 expression levels of WT and *Cdkl5*-null hippocampi at P>60. Tuj1 was used as loading control. **(D)** Densitometric quantification of data shown in C. Statistical analysis: unpaired Student's t test; sh#2 vs shLacZ: *p<0.05. (WT n=5; KO n=6).

3.6 Cdkl5 knock-down impairs membrane exposure of GluA2-containing AMPA receptors

To investigate if the altered AMPAR subunit expression can be mirrored in defective membrane insertion, surface and total staining of GluA1- and GluA2-containing receptors was performed. Immunofluorescence analyses of primary hippocampal neurons silenced for Cdkl5 at DIV0 were carried out at DIV18 with two different shRNAs (sh#1; sh#2) or shLacZ as control. When compared to control neurons, Cdkl5 silencing significantly reduced the amount of membrane-inserted GluA2-containing receptors (sh#1: 0.722±0.027, $p<0.001$; sh#2: 0.728±0.038, $p<0.001$), whereas the levels of membrane-inserted GluA1-containing receptors were unaffected (sh#1 0.920±0.068; sh#2 0.932±0.087; $p=0.548$) **(Fig. 6A-B)**. This result may be the reflection of the decreased amount of GluA2 total protein content described above. Nevertheless, when normalizing the surface pool of GluA2 to the total one, expressed as the ratio between surface and total amount of AMPA receptors, we also found a significant reduction in neurons silenced for Cdkl5 (sh#1: 0.775±0.043, $p<0.05$; sh#2: 0.698±0.066, $p<0.01$). Conversely, surface-to-total ratio of GluA1 was unaffected in Cdkl5-silenced neurons (sh#1 1.133±0.080; sh#2 1.053±0.165; $p=0.609$) **(Fig 6A-C)**. Altogether, this indicates that CDKL5 deficiency brings not only to a defect in GluA2 expression but also in its specific surfacing and recycling back to the membrane.

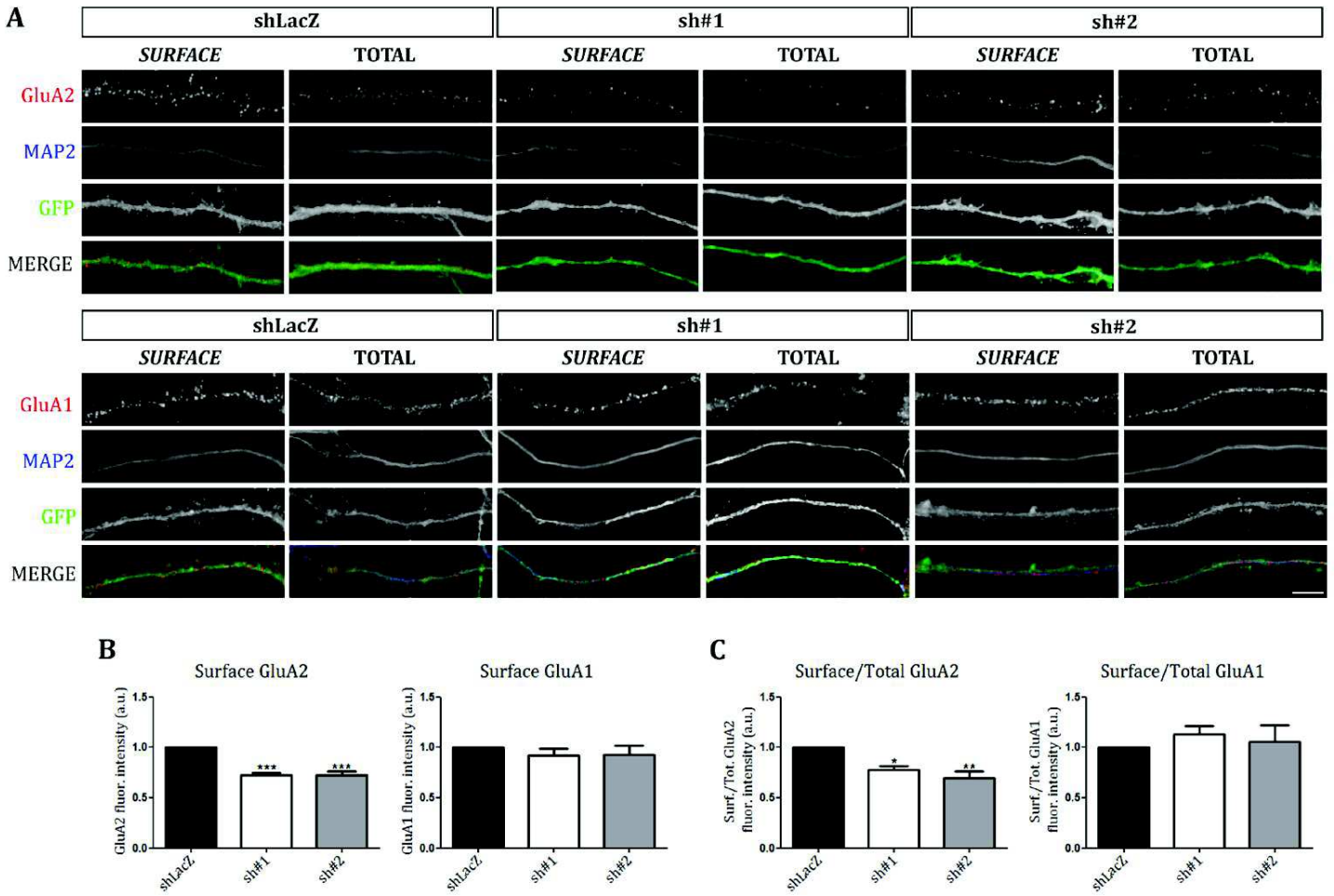

Fig. 6| Cdkl5 knock-down impairs membrane exposure of GluA2-containing AMPA receptors. (A) Representative images of surface and total fluorescence intensity of GluA1 and GluA2 in primary hippocampal neurons at DIV18 silenced for CDKL5 (sh#1 and sh#2) or, as control, shLacZ. For cell surface staining antibodies raised against extracellular epitopes were used under no-permeabilizing conditions. Scale bar 15 µm. **(B-C)** Quantification of data shown in A; GluA1 and GluA2 immunofluorescence intensities were analyzed on MAP2+ and GFP+ segments of dendritic branches. The surface-to-total ratio was calculated as the ratio between surface and total GluA1-GluA2 fluorescence intensities from single experiments. Analyses of n>4 independent experiments, n>20 segments/experiment; Statistical analysis: One-way ANOVA followed by Dunnett's multiple comparison test; shCdkl5 vs shLacZ: *p<0.05; **p<0.01; ***p<0.001.

3.7 Cell-surface biotinylation assays confirm defective AMPAR expression in Cdkl5-silenced neuronal cultures

Cell-surface biotinylation provides a highly sensitive and convenient method to label and recover cell surface exposed proteins. We exploited this approach to further confirm the altered membrane abundance of AMPA receptors in Cdkl5-deficient cultures. Cell-surface biotinylation was performed on primary hippocampal neurons silenced for Cdkl5 expression from DIV0-18 with sh#2, or shLacZ as control. Biotinylated proteins were recovered and analysed by WB in parallel with a fraction of the total protein extract. The amount of surface and total GluA2/GluA1 expression was analysed by Western blotting using the signal of GAPDH as internal loading standard. In line with the immunofluorescence studies, Cdkl5-silencing dramatically reduced GluA2 surface expression compared to control (sh#2: 0.173±0.027, $p<0.001$), while GluA1 surface expression showed a lesser but significant decrease (sh#2: 0.573±0.109, $p=0.017$) **(Fig. 7A-B)**. As expected, Cdkl5 knock-down also resulted in a significant alteration of the surface-to-total ratio of GluA2 (sh#2: 0.690±0.038, $p<0.001$), calculated as the ratio between biotinylated GluA2 and total protein extract. Even if the surface-to-total ratio of GluA1 was decreased it did not reach statistical significance (sh#2: 0.710±0.104, $p=0.052$) **(Fig 7A-C)**. These data confirm a role of CDKL5 in modulating both expression and surfacing of GluA2-containing receptors. Moreover, it is worth noting that Cdkl5-silencing resulted also in an altered subunit composition of surface exposed AMPA receptors. Indeed, by comparing the ratio between biotinylated GluA2 and GluA1 subunits in shLacZ and shCDKL5 neurons, we found that AMPARs in neurons devoid of CDKL5 are deprived of membrane GluA2 (sh#2: 0.313±0.064, $p<0.001$) **(Fig 7A-D)**. Considering that the presence of GluA2 plays a crucial role in rendering AMPARs impermeable for calcium ions our data suggest that the absence of CDKL5 may significantly alter neuronal calcium permeability.

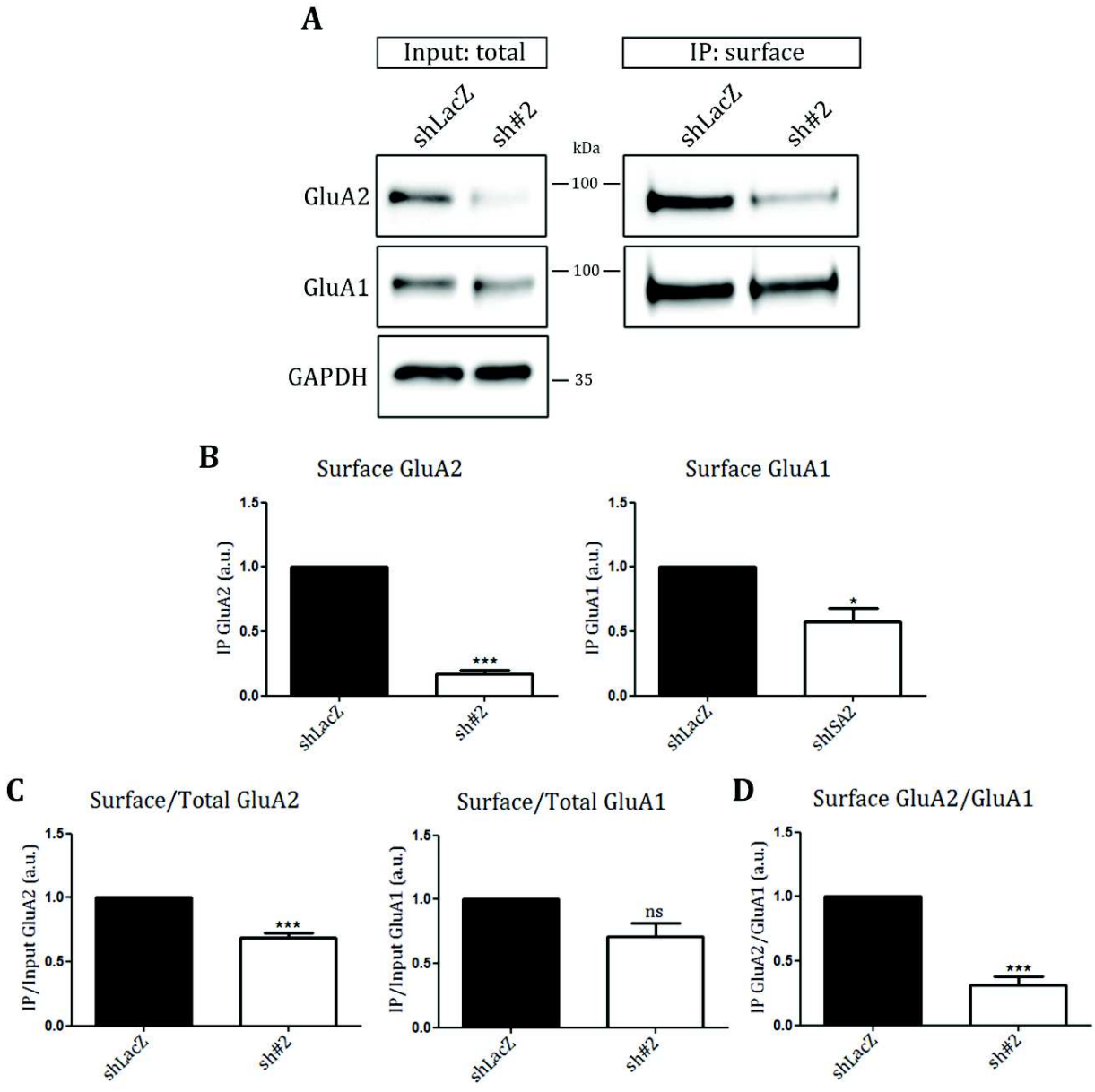

Fig. 7| Cell-surface biotinylation assay show altered membrane expression and composition of AMPARs in Cdkl5-silenced neurons. (A) WB showing GluA2/GluA1 levels in membrane fractions or total extracts of primary hippocampal neurons (DIV18) silenced for CDKL5 (sh#2) or, as control, shLacZ. Membrane fractions were purified by biotinylation. GAPDH was used as internal standard. **(B-D)** Densitometric quantification of data shown in A. Analysis of n=3 independent experiments. Statistical analysis: unpaired Student's t test; sh#2 vs shLacZ: *p<0.05; ***p<0.001.

3.8 Calcium imaging reveals an increased calcium influx through AMPARs in Cdkl5-deficient neurons

The depletion of GluA2-containing AMPARs at the neuronal membrane in CDKL5-deficient neurons that we observed above is likely to lead to increased calcium permeability. Thus, we exploited calcium imaging assays at DIV16 on primary hippocampal neurons silenced for Cdkl5 expression at DIV0 with sh#2, or LacZ, as control. Intracellular calcium levels were evaluated in resting neurons after the incubation with the fluorescent calcium sensor Rhod-3. We analysed infected neurons expressing GFP **(Fig. 8A)** by measuring the area under the curve (AUC) (represented in **Fig. 8B**) of Rhod-3 fluorescence intensity in a selected region of the soma (ROI) during a fixed time period. To prevent calcium influx from NMDARs, the extracellular solution was supplemented with 100 μM of the NMDAR antagonist APV. The results showed that Cdkl5-silenced neurons display significantly higher Rhod-3 levels corresponding to an increased calcium influx through AMPARs (sh#2: $4.870x10^4 \pm 1.013x10^4$ vs shLacZ: $2,445x10^4 \pm 4.762x10^3$, p=0.025) **(Fig. 8C)**; this altered calcium conductance strongly support a CDKL5-dependent derangement of surface AMPAR composition.

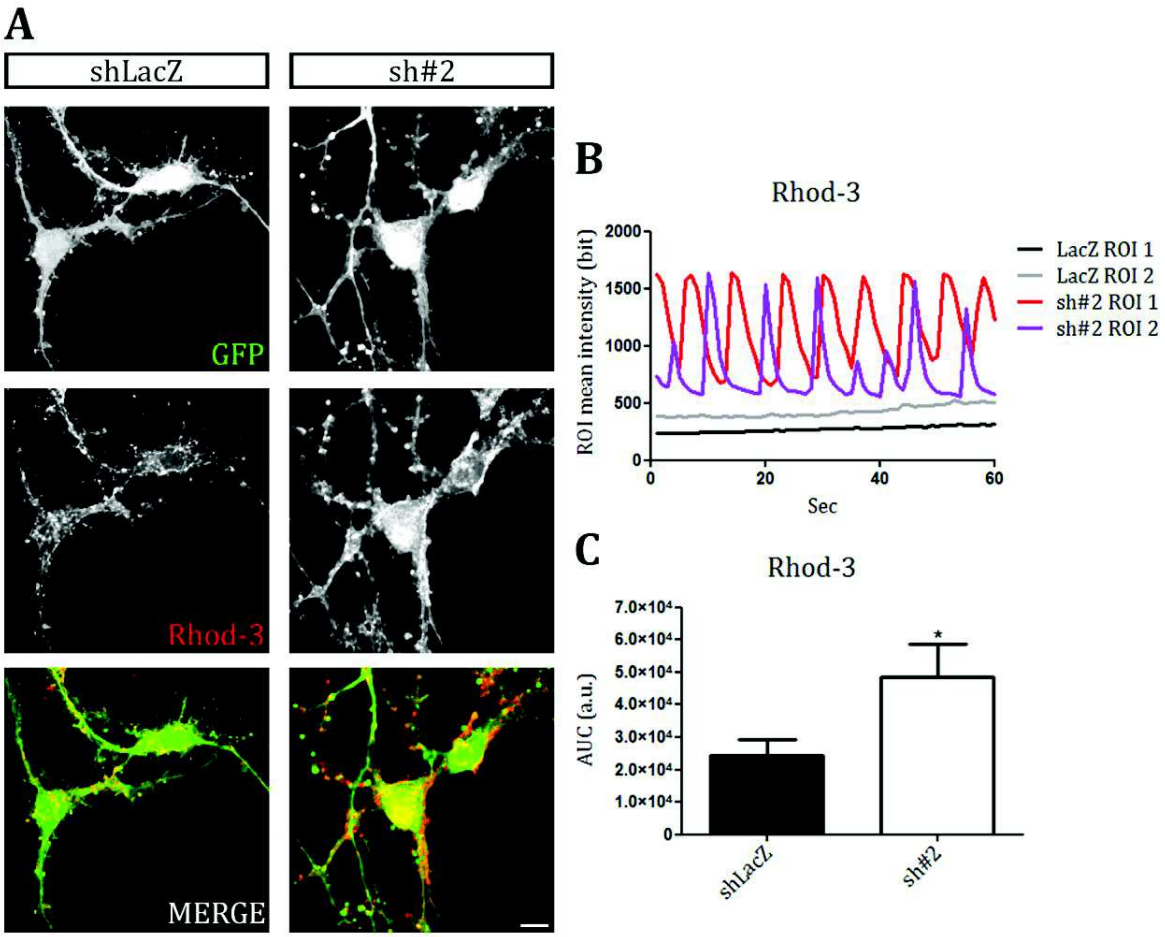

Fig. 8| Calcium influx through AMPARs is increased in Cdkl5-deficient neurons. (A) Representative frames showing Rhod-3 fluorescence intensity of GFP+ neurons silenced for CDKL5 (sh#2) or LacZ, as control. Scale bar 5 µm. **(B)** Representative levels of Rhod-3 fluorescence intensity of selected ROIs over 60 s. **(C)** Quantification of data shown in (B) expressed as the area under the curves (AUC), calculated as an integral of Rhod-3 fluorescence intensity over 60 s. Analysis of n>7 neurons per condition from 2 different replicates. Statistical analysis: unpaired Student's t test; sh#2 vs shLacZ: *p<0.05.

3.9 Cdkl5 silencing alters spine number and morphology

Growing pieces of evidence suggest that loss of CDKL5 leads to alterations of spine number and morphology both *in vivo* and *in vitro.* AMPAR deregulation, as observed in our Cdkl5-silenced cultures, may contribute to those alterations since several studies revealed the importance of GluA2-containing AMPARs for proper spine formation and development (*59*). As expected, primary hippocampal neurons silenced for Cdkl5 with two different shRNAs (sh#1; sh#2) were characterized by altered spine density and morphology when compared to control neurons. In particular, silencing of CDKL5 caused a significant decrease of spine number at DIV18 (sh#2: 4.770±0.650 vs shLacZ: 7.646±0.786, $p<0.05$; sh#1: 5.697±0.450 vs shLacZ, $p>0.05$) **(Fig. 9C)**. The degree of spine maturation can be defined through morphological parameters. In particular, filopodial, thin e stubby spines are considered immature spines, whereas mushroom and cup-shaped spines are defined as mature spines. Morphological classification of spines in Cdkl5-deficient neurons revealed a significant increase in the presence of immature spines (sh#1: 82.76±2.692 vs shLacZ: 43.10±3.357, $p<0.001$; sh#2: 87.81±3.456 vs shLacZ, $p<0.001$) along with a decreased expression of mature spines (sh#1: 17.24±2.692 vs shLacZ: 56.90±3.357, $p<0.001$; sh#2: 12.19±3.456 vs shLacZ, $p<0.001$) **(Fig. 9D)**.

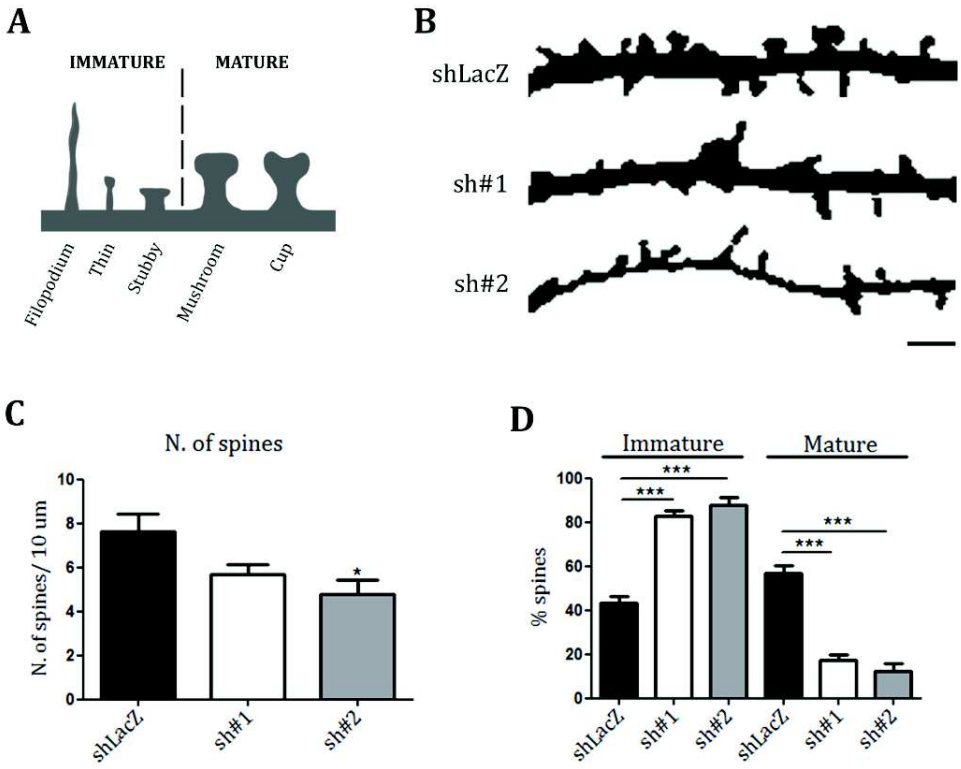

Fig. 9| Cdkl5 knock-down causes altered spine number and morphology. (A) Representative image showing the classification of spine maturation based on morphology. Filopodial, thin and stubby spines were classified as immature spines, whereas mushroom and cup spines were classified as mature spines. **(B)** Representative image showing spine density and morphology of Cdkl5-silenced cultures with sh#1 and sh#2 or shLacZ. Scale bar 2 µm. **(C)** Quantification of spine density of neurons showed in (B). Spine density was calculated as the number of spines in 10 µm dendritic segments. **(D)** Morphological classification of spines showed in (B) using the criteria reported in (A). Spine analyses were performed using GFP expression as reporter of lentiviral infection. Analyses of 24 dendritic segments from 2 independent experiments. Statistical analysis: One-way ANOVA followed by Dunnett's multiple comparison test; shCdkl5 vs shLacZ: *p<0.05; ***p<0.001.

3.10 Wild type CDKL5, but not pathological mutants, promotes surface expression of homomeric GluA2 AMPA receptors in COS7 cells

To further investigate the role of CDKL5 in influencing membrane insertion of AMPARs, we utilized COS7 cells that were co-transfected with constructs encoding GFP-GluA2 or GFP-GluA1 along with *wild type* Flag-CDKL5_1. Immunofluorescence analysis revealed that, despite the successful expression of both GFP-GluA2 and GFP-GluA1 in COS7 cells, only GFP-GluA2 homomers can undergo membrane insertion **(Fig 10A-B)**. Endogenous CDKL5 is detectable in COS7 cells, but at relative low levels compared to neurons and brains (data not shown). Despite that, endogenous CDKL5 exert a biological function in this cell line as its silencing disrupt the mitotic spindle leading to altered mitosis (Chandola C. et al., under revision), as well as alterations in cytoskeleton organization and cell morphology (Barbiero I. et al., submitted). Interestingly, GFP-GluA2 surface expression was significantly enhanced by Flag-CDKL5 co-transfection (Ctrl vs CDKL5 $p<0.05$) **(Fig. 10C)**, consistently with a role of the kinase in GluA2 membrane insertion. In parallel, we also expressed three different pathological CDKL5 derivatives: A40V and C152F are characterized by reduced catalytic activity, whereas the truncated derivative Δ781 has increased catalytic activity and is constitutively confined within the cell nucleus **(Fig. 10A)**. Of note, neither of these derivatives were capable of increasing GFP-GluA2 membrane insertion ($p>0.05$) **(Fig. 10C)**, indicating that this property of CDKL5 is lost both in case of missense and truncating pathological mutations. Altogether, these results suggest a possible role of functional CDKL5 in regulating GluA2-containing AMPA receptor trafficking towards the cell membrane. Further analyses will be aimed to investigate the role of pathological CDKL5 derivatives in neuronal cultures, as well as their capacity to rescue the AMPARs defects.

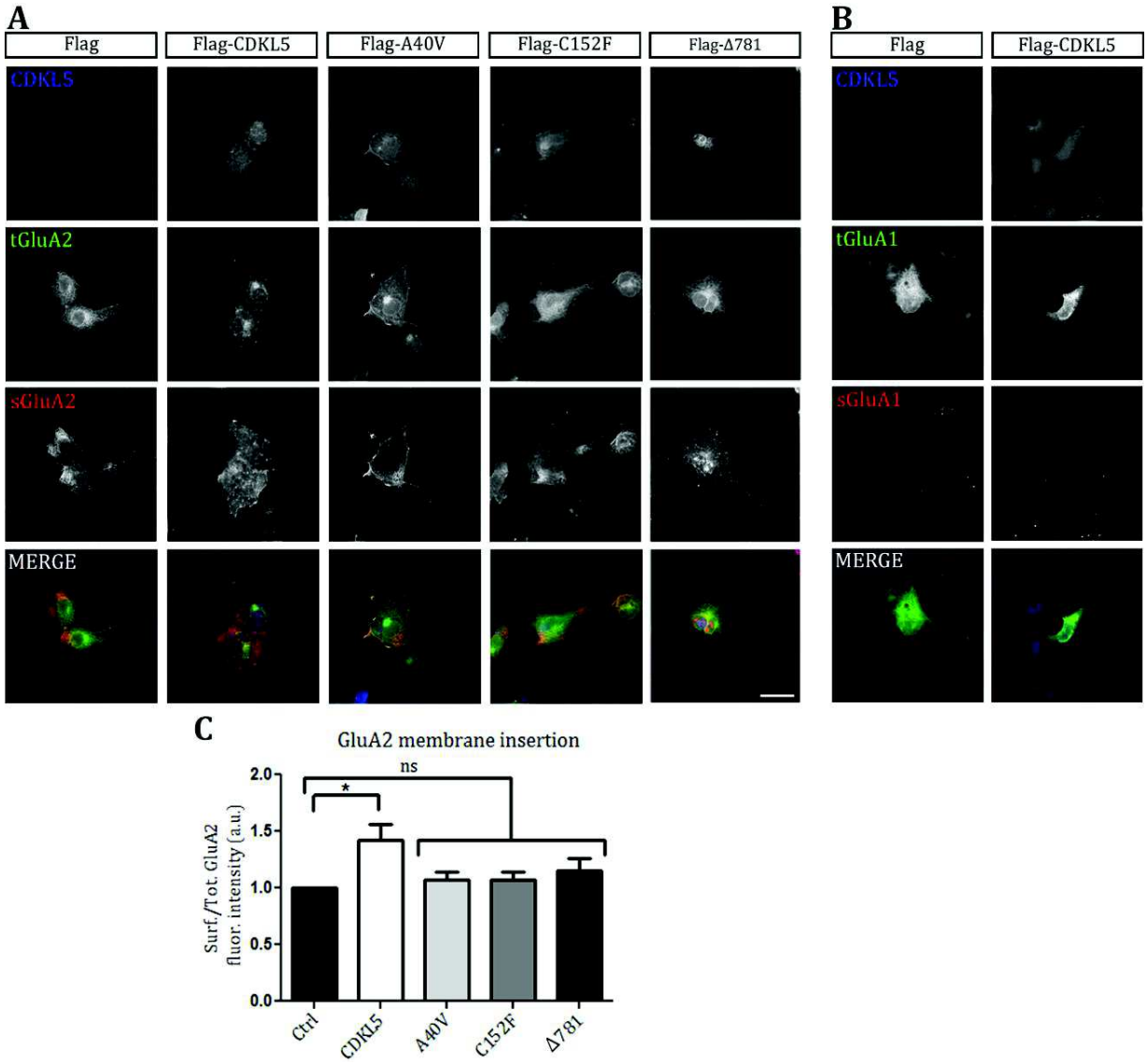

Fig. 10| CDKL5 promotes surface expression of homomeric GluA2 AMPA receptors in COS7 cells. (A) Representative images of immunofluorescent staining for surface and total GFP-GluA2 co-overexpressed with wild type Flag-CDKL5 or the indicated pathological derivatives in COS7 cells. Scale bar 20 µm. **(B)** Representative images of surface and total fluorescence staining of GFP-GluA1 co-overexpressed with Flag-CDKL5 in COS7 cells. For cell surface staining, an antibody raised against an extracellular epitope of GluA2 (sGluA2) or GluA1 (sGluA1) was used under non-permeabilizing conditions followed by incubation with antibodies against either GFP or CDLK5 in a permeabilizing buffer to detect respectively total GluA2 (tGluA2) and CDKL5 overexpression. **(C)** Quantification of data shown in A. The surface-to-total ratio was calculated as the ratio between surface and total GluA2 fluorescence intensities from a single experiment. Analysis of n>3 independent experiments; Statistical analysis: One-way ANOVA followed by Dunnett's multiple comparison test; *p<0.05.

3.11 GRASP-1 is a novel interactor of CDKL5

The knowledge of the interacting partners of CDKL5 constitutes a fundamental tool to understand the functions of CDKL5 and to predict the biological processes in which the kinase is involved. To this end, a Yeast Two-Hybrid (Y2H) screening had previously been performed in our laboratory in which the C-terminal tail of hCDKL5_5 (AA 299-1030) was used as bait to screen a human adult brain cDNA library. Among the 171 interacting clones that were identified, GRASP-1 caught our interest. GRASP-1 is a neuronally-enriched protein that was initially isolated as a GRIP1-interacting factor. GRASP-1 has two distinct roles in neuronal functions: it is required for proper AMPAR recycling and it is critical for spine morphology. The CDKL5 interaction surface within GRASP-1 is localized in the C-terminal region (amino acids 588-797) **(Fig. 11A)**. The interaction between CDKL5 and GRASP-1 was further confirmed by co-immunoprecipitation experiments both *in vitro* and *in vivo*. In particular, Flag-CDKL5 and GFP-GRASP-1 co-immunoprecipitate from overexpressing HEK293T cells **(Fig. 11B)**. This result was replicated also with transfected COS7 cells (data not shown). Importantly, when CDKL5 was immunopurified from P25 mouse brain lysates, we could also detect GRASP-1 in the pellet. Interestingly, also Syntaxin 13 co-immunoprecipitated with CDKL5. Syntaxin 13 is an endosomal SNARE protein involved in recycling of endosomal domains and an already known interactor of GRASP-1 **(Fig. 11C)**. These results suggest that CDKL5 may participate in a molecular complex that regulates endosomal sorting towards the neuronal membrane.

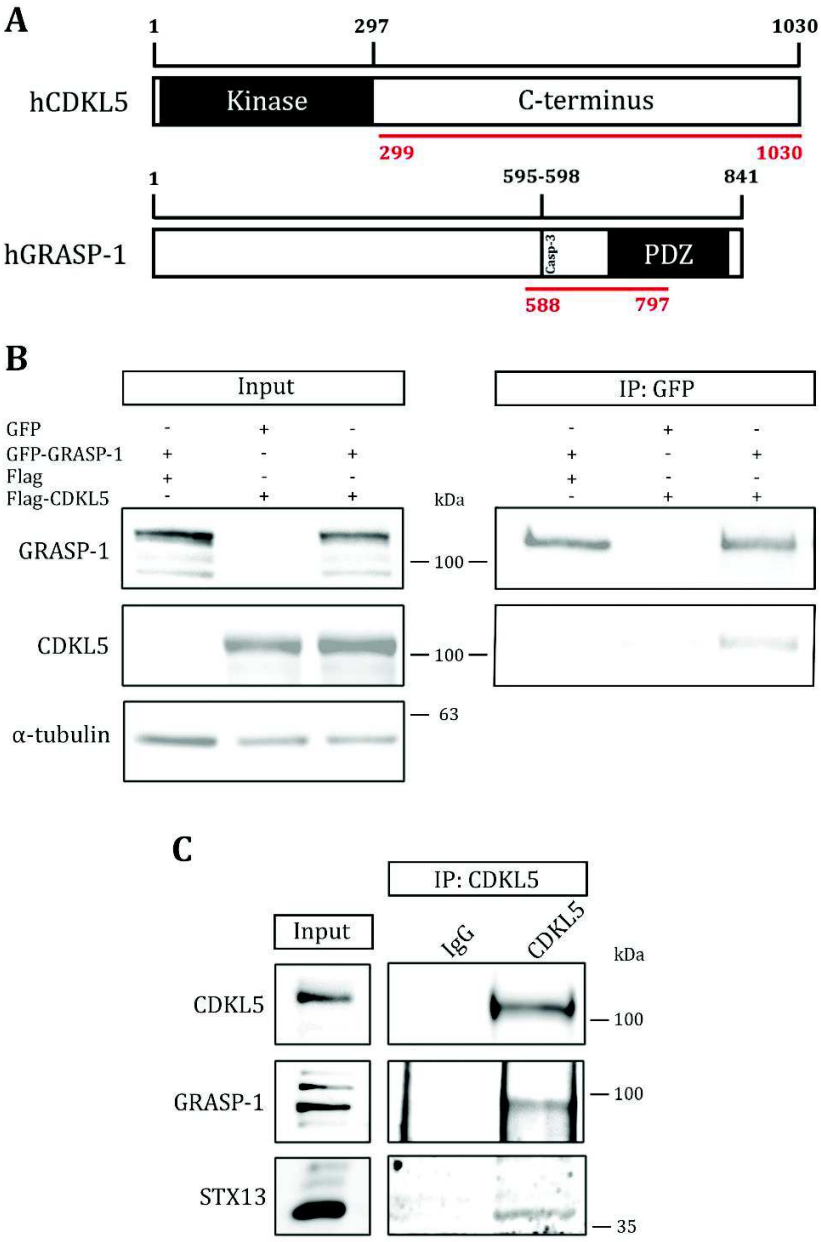

Fig. 11| GRASP-1 is a novel interactor of CDKL5. (A) Schematic representation of hCDKL5_5 and hGRASP-1 with the functional domains and signatures indicated. Casp-3: Casapse-3 cleavage-site; PDZ-like domain. The C-terminal region of hCDKL5_5 spanning amino acids 299-300 (upper red line) was used as a bait. The region encompassing amino acids 588-797 of hGRASP-1 (lower red line) was found to interact with CDKL5. **(B)** Co-immunoprecipitation of HEK293T cells transfected with the indicated proteins. Whole cell lysates were incubated with anti-GFP antibodies and immunocomplexes and inputs (5% of IP) were evaluated by Western blotting using the signal of α-tubulin as internal standard. (n=3). **(C)** Representative co-immunoprecipitation experiment of P25 mouse brain lysates with anti-CDKL5 antibody or unrelated IgGs. Co-immunoprecipitates and inputs (5% of IP) were evaluated by Western blotting analysis. STX13: Syntaxin 13. (n=3).

3.12 The phosphorylation status of GRASP-1 changes during brain development

Considering the interaction between CDKL5 and GRASP-1, we hypothesize that the latter may be a substrate of the catalytic activity of CDKL5. To date, several serine and threonine residues in GRASP-1 have been identified as being phosphorylated in both human and mouse brain; however, no reports have so far described a direct involvement of CDKL5 (www.phopshosite.org) (*112*). To analyze the phosphorylation status of GRASP-1 during development, we performed two-dimensional gel electrophoresis on P5 and P25 wild type mouse brain lysates. The basic shift of GRASP-1 in λ-phosphatase (λPP)-treated P5 brain lysates suggested the existence of at least one phosphorylated isoform of the protein. Interestingly, at P25, much more acidic GRASP-1 isoforms appeared with respect to P5, suggesting an increase of its phosphorylation profile in the more mature brain **(Fig. 12)**; this is in accordance with the concomitant increasing expression of CDKL5 during early brain development.

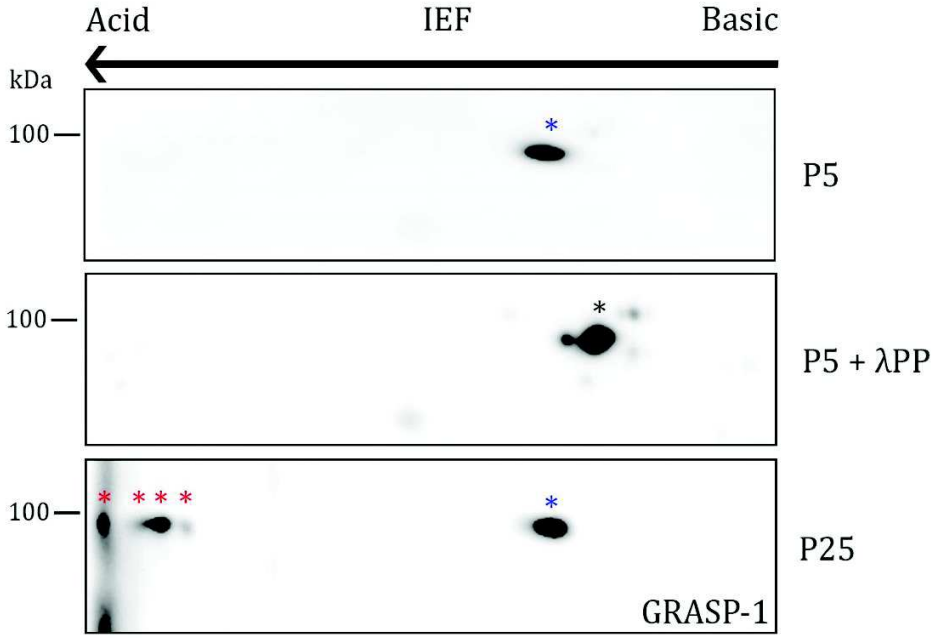

Fig. 12| GRASP-1 phosphorylation changes during brain development. WB showing two-dimensional gel electrophoresis of P5 and P25 mouse brain lysates. A P5 brain extract was treated with or without lambda phosphatase (λPP). GRASP-1 was detected by immunoblotting; the single spot of intermediate filament NFL was used as internal control for alignment (data not shown). λPP treatment resulted in a basic shift of GRASP-1 isoform/s (black asterisk compared to blue asterisks). At P25 an increased number of GRASP-1 acidic spots (red asterisks) were present as compared to P5. (n=1).

3.13 Tianeptine normalizes GluA2 subunit expression and S880 phosphorylation in Cdkl5-deficient cultures

Tianeptine (S 1574, [3-chloro-6-methyl-5,5-dioxo-6,11-dihydro-(c,f)-dibenzo-(1,2-thiazepine)-11-yl) amino]-7 heptanoic acid, sodium salt) is an anti-depressant with known memory-enhancing effects as its administration increases long-term memory in rodents (*113*, *114*). Of relevance for our purpose, tianeptine has been found to greatly stabilize surface AMPARs at the synaptic sites by reducing their surface diffusion through a CamKII-stargazin-PSD-95 pathway (*115*). Although the molecular mechanisms by which tianeptine favours synaptic plasticity are not known, it is likely to involve the dynamic retention of surface AMPARs at the synapse. Against this background, the pharmacological potential of tianeptine was tested on the AMPAR defects observed in our Cdkl5-silenced neuronal cultures. To this aim, Cdkl5-interfered neurons were treated at DIV11 with 10 μM of tianeptine, which was replenished every second day till DIV18, when neurons were harvested and processed for SDS-PAGE and Western blotting analysis. Importantly, tianeptine treatment completely restored GluA2 expression (sh#2: 0.553±0.045 vs shLacZ, $p<0.001$; sh#2+TIA: 1.067±0.267 vs sh#2, $p<0.001$; sh#2 vs shLacZ, $p>0.05$) and reduced S880 phosphorylation (sh#2: 1.952±0.124 vs shLacZ, $p<0.001$; sh#2+TIA: 1.340±0.196 vs sh#2, $p<0.05$; sh#2 vs shLacZ, $p>0.05$) in neurons silenced for Cdkl5 compared to controls **(Fig. 13 A-B)**. These results place tianeptine as an interesting candidate drug for CDKL5 disorder.

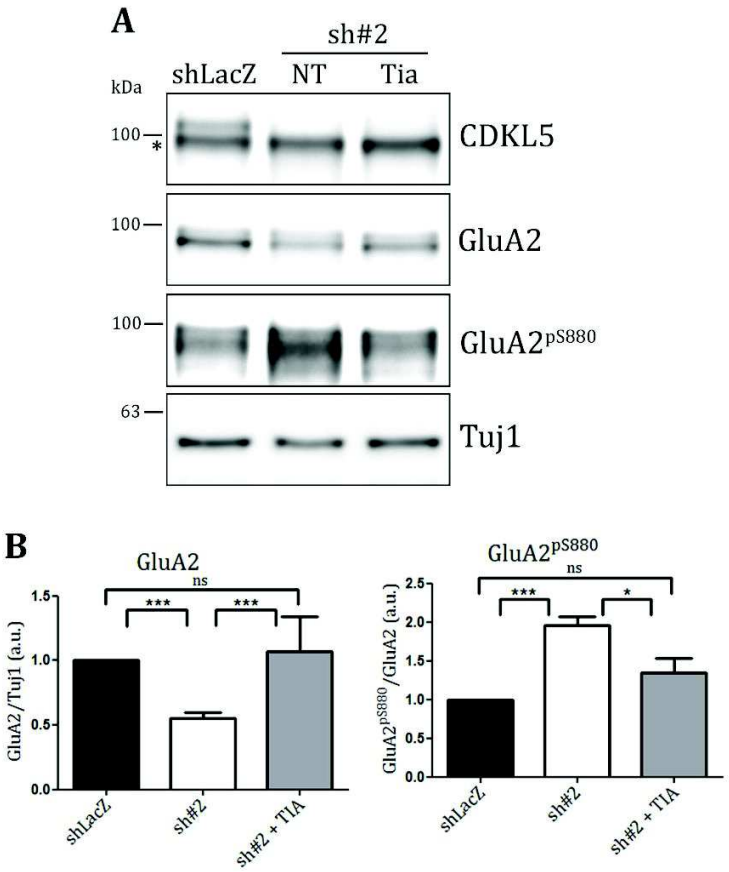

Fig. 13| Tianeptine completely normalizes GluA2 subunit expression and S880 phosphorylation in Cdkl5-deficient cultures. (A) WB showing GluA2 and S880 phosphorylation in primary hippocampal neurons silenced for Cdkl5 (sh#2), treated with 10 μM tianeptine for 7 days and harvested at DIV18. TUJ1 was used as loading control. Black asterisk indicates a non-specific signal in CDKL5 immunoblot. **(B)** Densitometric quantification of data shown in A. GluA2^{pS880} was evaluated as the ratio between phosphorylated and total GluA2 levels. (n=3). Statistical analysis: One-way ANOVA followed by Tuckey's multiple comparison test; *p<0,05; ***p<0,001.

4. DISCUSSION

Mutations in the X-linked Cyclin-dependent kinase-like 5 (*CDKL5*) gene have been linked to human neurological disorders such as early epileptic encephalopathy and the Hanefeld variant of Rett syndrome (RTT) (*14*) that share as common features the early onset of intractable seizures, severe intellectual disability, autistic traits, hypotonia and some RTT-like features such as hand stereotypies. Today, however, clinicians agree that the peculiar pattern of clinical presentations in *CDKL5*-mutated individuals represent an independent clinical entity, named *CDKL5 disorder* (*8*, *9*).

In line with its role in the nervous system, CDKL5 levels are highest in brain where its timing of expression correlates with synaptogenesis (*18*). Several data link CDKL5 with dendritic spine development and synaptic activity. The protein is synthesized locally in spines upon neuronal activity suggesting that it may have several targets in synaptic structures (*15*). In spines, CDKL5 promotes synaptic stabilization by associating with the post-synaptic scaffolding protein PSD95 and phosphorylating NGL1 (*28*, *29*). Importantly, *Cdkl5*-null mice and silenced neurons display decreased spine density as result of impaired spine stabilization, defective excitatory activity and impaired long-term potentiation (*28*, *29*, *32*, *33*). Moreover, loss of Cdkl5 in mice alters many signal transduction pathways, including that of AKT-mTOR, and the phosphorylation profile of some kinases, among which PKA, PKC, and PKD that are involved in synaptic plasticity (*30*). Overall, these data show the importance of CDKL5 for proper spine development and function but the molecular network through which CDKL5 governs these aspects is far from fully understood.

4.1 CDKL5 knock-down affects GluA2 expression and subunit composition of membrane-inserted AMPARs

Considering all the above, during my Ph.D. studies, I focused my attention on a key determinant of synaptic strength and plasticity, the AMPA receptor, the deregulation of which could underlie, at least in part, the synaptic defects associated with loss of Cdkl5.

To this aim, we took advantage of mouse primary hippocampal neurons silenced for Cdkl5-expression to study AMPAR expression and composition. Interestingly, we found that Cdkl5 knock-down resulted in a dramatic decrease in expression of the AMPAR subunit GluA2 in mature neurons, whereas GluA1 levels were unaltered.

It is worth noting that these results were mirrored by primary hippocampal neurons from *Cdkl5*-null embryos and *in vivo* in hippocampi from adult *Cdkl5*-null brains; this suggests that altered AMPAR subunit expression is specifically due to the loss of Cdkl5.

As demonstrated by qPCR analyses, GluA2 downregulation in Cdkl5-silcenced neurons is independent from its mRNA expression, and is thus likely to rely on post-transcriptional mechanisms. Among these, we focused our attention on GluA2 post-translational modifications that are widely known to regulate AMPAR dynamics and turnover. In particular, phosphorylation at serine 880 (S880) is known to be critical in controlling the fate of GluA2. GluA2 homomers, as well as GluA2/GluA3 heteromers, undergo exo- and endo-cytotic processes (*116*), which are influenced by the phosphorylation status of S880 that modulates the affinity of GluA2 for the PDZ-domain partners GRIP1/2 and PICK1 (*117*). Specifically, upon phosphorylation at S880 by PKC, the affinity of GluA2 for GRIP1/2, which stabilizes the surface expression of the receptor, is lost in favour of PICK1 binding that drives the receptor towards internalization, intracellular retention in nonrecycling compartments and/or lysosomal degradation. Interestingly, we found that Cdkl5 knock-down results in hyper-phosphorylation of S880 and in an increased co-localization between internalized GluA2 and the lysosomal marker LAMP-1, suggesting that reduced GluA2 levels may be due to increased degradation of intracellular-retained receptors. Whether other post-transcriptional mechanisms regulating GluA2 expression, besides lysosomal degradation, are targeted by CDKL5 is still to be investigated.

Besides the reduced levels of total GluA2 we also found a net loss of GluA2-containing synaptic AMPARs. As a matter of fact, Cdkl5-silenced neurons displayed an altered subunit composition of membrane-inserted AMPARs, which are deprived of GluA2 and thus enriched in GluA1. While GluA1 are calcium permeable and are important for the early phase of induction of LTP, the presence of GluA2 in heteromeric AMPARs renders the channel impermeable to calcium (Ca^{2+}), thus influencing channel kinetics, conductance and synaptic transmission (*53*, *54*) and are required for the maintenance of LTP (*118*). These speculations

are corroborated by our calcium imaging assays indicating that Cdkl5-deficient cultures are characterized by an increased AMPAR-dependent Ca^{2+} influx, which is likely to affect the signalling landscape and, thus, neuronal functionality. We can speculate that the unbalance of GluA1/2 subunits inserted into the post-synaptic membranes may be one of the molecular mechanisms that impair LTP maintenance as reported in the mouse model (*33*).

Several studies have linked the alteration of the relative proportion of Ca^{2+} permeable (CP)-AMPAR subunits with pathological states, including autism spectrum disorders and epilepsy. For instance, Rab39b-silenced mouse hippocampal neuron showed a reduction of GluA2-containing AMPARs at the post-synaptic membrane (*110*). Loss-of-function mutations in the X-linked *RAB39B* gene are associated with intellectual disability, autism spectrum and seizures (*119*). RAB39B is a RAB GTPase that has a key role in blocking the retention of GluA2/GluA3 heteromers in the endoplasmatic reticulum and promoting their translocation into the Golgi, hence leading to surface expression of Ca^{2+}-impermeable (CI) AMPARs (*110*, *119*).

It is striking that hippocampal pyramidal neurons from symptomatic *Mecp2*$^{-/-}$ mice, which recapitulate many features of Rett syndrome, display a preponderant expression of CP-AMPARs at the post-synaptic membrane. This is consistent with higher total and surface GluA1 levels, increased sensitivity to the CP-AMPAR selective inhibitor NASPM on AMPAR-mediated EPSCs, and their smaller inward rectification (*111*). The authors proposed a model in which higher GluA1 levels result from a gradual accumulation and impaired removal at the nascent synapses of *Mecp2*$^{-/-}$ hippocampal neurons. In particular, increased phosphorylation of GluA1 at serine 845, as well as increased expression of the membrane-anchoring molecule SAP97, stabilize GluA1 at the synaptic membrane, while the concomitant reduction of the early-endosomes molecule EEA1 leads to an impaired endocytosis. Despite that GluA2 expression levels and surface expression were not investigated in this work, it is worth to note that also in the murine model of Rett syndrome, a disease tightly linked to CDKL5 disorder, GluA2 is reduced in *Mecp2* knock-out hippocampal neurons and brains (*120*, *121*). Importantly, the increase of GluA1 in Mecp2$^{-/-}$ neurons may contribute to the unbalanced expression of CP/CI-AMPARs similarly to what occurs in our silenced neurons where, on the contrary, it is the GluA2 subunit to be depleted. It is thus plausible that these defects, despite opposite at the beginning, might converge to an overlapping outcome.

Overall, the above pieces of evidence have led to propose that the altered composition of membrane-inserted AMPARs, which lead to an increased Ca^{2+} permeability, are critical for the onset of several neurological features, such as cognitive impairment and seizures that characterize autism spectrum disorders and might thus represent the molecular basis for pathological outcomes also of CDKL5 disorder.

Loss of GluA2-containing AMPARs can affect not only the spine functionality, as shown above, but also spine number and morphology.

Several pieces of evidence suggest that the presence of GluA2 subunits in membrane-inserted AMPARs correlated with the number, size and shape of dendritic spines (*59*, *60*). In particular, silencing of GluA2 expression in mouse primary hippocampal neurons causes a significant reduction of spine density and width, whereas GluA2 overexpression in mature neurons increases spine number as well as their size. Surprisingly, neither GluA1 nor GluA3 overexpression affects the size or number of dendritic spines, suggesting that the spine-promoting activity seems to be specific for GluA2.

On that basis, it is tempting to link the reduced spine density and the high degree of spine immaturity characterizing not only Cdkl5 deficient neurons (*32*, *33*) to the impaired expression of GluA2. Analogously, impaired surface expression of GluA2-containing AMPARs in primary hippocampal neurons by the silencing of the autism-related gene *Rab39b* affected spine length and width.

4.2 CDKL5 is involved in molecular pathways that regulate the membrane insertion and recycling of GluA2-containing AMPARs

Cdkl5-silenced cultures displayed a reduced surface to total ratio of GluA2-containing AMPARs, suggesting that loss of Cdkl5 can impair the trafficking of the receptor towards the membrane and thereby lead to depletion of synaptic GluA2.

Interestingly, overexpression of CDKL5 in COS7 cells is sufficient for enhanced membrane insertion of exogenously expressed GluA2-homomers. This effect cannot be obtained by pathological derivatives of CDKL5 such as A40V, C152F and Δ781. Previous *in vitro* analysis from our laboratory showed that the C152F (*122*) and A40V (unpublished data) derivatives are devoid of catalytic activity (*24*). Conversely, the truncated derivate Δ781 (R781X) showed an increased kinase activity together with a constitutive nuclear localization (*18*). These data

suggest that both the kinase activity and the cytoplasmic localization of CDKL5 are necessary for promoting the membrane insertion of GluA2-homomers in COS7 cells.

A previous yeast two-hybrid (Y2H) screening revealed that the C-terminus of CDKL5 can hypothetically interact with GRASP-1, a component of the molecular machinery that regulates the directionality of endosomal trafficking in neurons. GRASP-1, also known as GRIPAP-1 (GRIP1 Associated Protein 1), is a neuron-enriched protein that was found as an interactor of the seven PDZ domain-containing scaffolding protein GRIP1 (*123*), which transports and stabilizes GluA2 containing AMPARs at synapses. Despite that GRASP-1 was originally found to act as a neuronal Ras GEF *in vitro* (*123*), recent conflicting data did not find either detectable GEF activity for Ras *in vivo*, or homology with known rasGEF domains (*124*). Differently, Hoogenraad and colleagues proposed GRASP-1 as a novel Rab4 effector (*124*). The endosomal Rab proteins (Rab5, Rab4, and Rab11) have all been implicated in endosomal receptor trafficking (*125*, *126*). Rab5 controls the transport to early endosomes/sorting endosomes, whereas Rab4 and Rab11 are involved in the regulation of endosomal recycling back to the plasma membrane (*127*). GRASP-1 was found to be an effector of Rab4, coordinating the route of endosomal recycling towards the plasma membrane by coupling Rab4-positive endosomes with Rab11-positive recycling endosomes. Since GRASP-1 cannot bind directly Rab11, the endosomal coupling is mediated by its interaction with an other component of the recycling endosomes, syntaxin 13 (STX13). Indeed, STX13 is enriched in Rab11 endosomal fractions and, importantly, is a key component of the SNARE core complex involved membrane fusion. Hoogenraad et al. proposed a model in which GRASP-1 binds the active form of Rab4 via its N-terminus and promotes the fusion with Rab11-positive endosomes binding STX13 via its C-terminus. As a matter of fact, mutations in STX13 separate Rab11-positive recycling endosomes from Rab4/GRASP-1-positive endosomes. Interestingly, GRASP-1 was found to co-localize with internalized AMPARs and GRASP-1 knock-down decreased the recycling of GluA2 subunit after AMPA stimulation leading to endosomal exit routes, specifically, towards lysosomal degradation; a similar defect is plausible also when CDKL5 is missing, as suggested by our data. Moreover, similarly to CDKL5, GRASP-1 silencing decreased the total number of synaptic protrusions and mushroom-shaped spines and impairs the late phase of LTP in hippocampal slices.

In line with the evident role of GRASP-1 for synaptic activity, the *GRASP-1* gene has been proposed as a novel X-Linked Intellectual Disability (XLID) gene (*128*). Indeed, duplication of a region of Xp11 containing *GRASP-1,* has been associated with autism with severe intellectual disability (*129*, *130*).

Our analyses showed that CDKL5 and GRASP-1 interact both *in* vitro and *in vivo*. Interestingly, also STX13 co-immunoprecipitated with Cdkl5 *in vivo* suggesting that Cdkl5, along with GRASP-1 and STX13, may participate in the molecular complex involved in Rab4/Rab11 endosomal coupling. Considering the interaction between CDKL5 and GRASP-1, we speculate that the latter may be a substrate of the catalytic activity of CDKL5, although no reports have so far described GRASP-1 phosphorylation. Our preliminary studies indicate that phosphorylation of GRASP-1 increases during early brain development concomitantly with increased expression of CDKL5 (*18*). Given the role of GRASP-1 in spines and its increase in phosphorylation during the peak of synaptogenesis (*131*), it is tempting to speculate that GRASP-1 phosphorylation is involved in spine development and functionality. We therefore find it challenging to address in future studies of *Cdkl5*-null brains if GRASP-1 is a substrate of CDKL5 and if the overlapping phenotypes induced by the absence of either CDKL5 or GRASP1 indicate a molecular link between the two proteins.

It worth noting that the Y2H screening assay revealed that CDKL5 interacts with a region of GRASP-1 covering a caspase-3 cleavage site ($D^{595}TVD^{598}$). An additional regulation of GRASP-1 by caspase-3 cleavage (*123*, *132*) could separate the N-terminal Rab4 binding domain from the C-terminal STX13 binding site, potentially disrupting the coupling between Rab4 and Rab11 endosomes. In this regard, CDKL5 binding at the cleavage site, possibly involving an event of phosphorylation, could hypothetically protect GRASP-1 from cleavage and thereby promote endosomal recycling of GluA2 towards the plasma membrane.

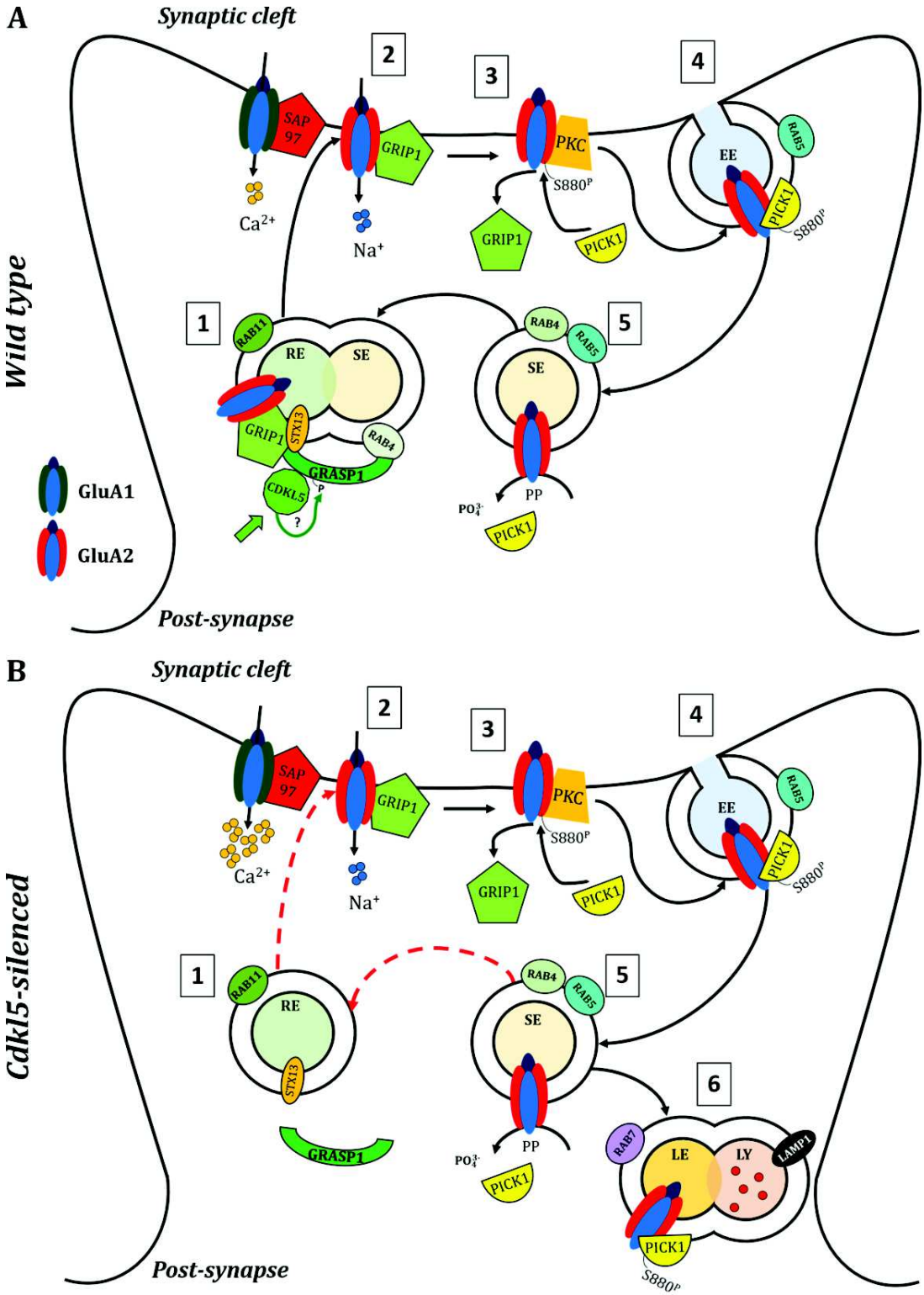

Image 3| Proposed working model of CDKL5 function in AMPAR composition. A (1-2) GRASP-1 mediates the endosomal coupling between Rab4 sorting endosomes (SE) an Rab11 recycling endosomes (RE) acting as a

molecular bridge between Rab4 and STX13. We proposed CDKL5 as a novel interactor of GRASP-1 which may participate in the molecular complex that promotes the surface insertion of GluA2-containing AMPARs. **(3-4)** GluA2-containing AMPARs undergo constitutive recycling. Upon phosphorylation at S880 by PKC, GluA2 affinity for GRIP-1 is lost in favour of PICK1 which promotes receptor internalization in Rab5 early endosomes (EE). **(5)** Once dephosphorylated, internalized GluA2 undergoes recycling back to the post-synaptic density by the interaction with the molecular complex involving GRASP-1 and its binding partners. **B (1-2)** The absence of CDKL5 may disrupt Rab4/Rab11 endosomal coupling, leading to the depletion of CI-GluA2-containing AMPARs at post-synaptic sites. **(3-6)** The impairment of endosomal recycling back to the membrane drives internalized GluA2 towards the endosomal exit route via Rab7 late endosomes (LE) and LAMP-1 lysosomes (LY), where it is finally degraded.

To date, no cure exists for CDKL5 disorder and therapies are only aimed at alleviating symptoms. The rational design of therapeutic strategies is still hindered by the limited knowledge of CDKL5 functions underscoring the importance of unravelling the neuronal functions of this kinase.

The findings described above show that loss of Cdkl5 causes a decreased expression of total and surface GluA2 AMPAR subunit that appears to rely on impaired membrane insertion and increased degradation. These alterations may explain several neurological features, such as cognitive impairment and seizures, that characterize CDKL5 disorder.

4.3 Tianeptine is a promising drug for CDKL5-associated AMPAR defects

An important aspect is whether these defects may represent novel targets for therapeutic intervention. On that basis, we focused our attention on tianeptine, a promising drug that was reported to modulate AMPAR-mediated glutamatergic neurotransmission.

Tianeptine, [3-chloro-6-methyl-5,5-dioxo-6,11-dihydro-(c,f)-dibenzo-(1,2-thiazepine)-11-yl) amino]-7 heptanoic acid sodium salt, is an antidepressant with structural similarities to the tricyclic antidepressant agents but with different pharmacological properties, which challenge the traditional monoaminergic hypothesis of depression. Extensive studies revealed that tianeptine has no significant binding affinity for classical anti-depressant drug-directed targets, including 5-HT receptors, dopamine receptors, adrenoceptor, glutamate receptors and monoamine transporters (*133*). Since several studies revealed that the glutamatergic signalling is impaired in depressed individuals (*134*) and that the treatment

with classic antidepressants, such as the selective serotonin reuptake inhibitor fluoxetine and the monoamine reuptake inhibitor imipramine, potentiate the phosphorylation of AMPAR (*135*, *136*), it is likely that the modulation of glutamatergic neurotransmission can be linked to the therapeutic impact of the antidepressant.

Tianeptine is classified as a glutamatergic antidepressant as it can potentiate AMPAR signalling by activating CaMKII and PKA via the p38, p42/44 MAPK and JNK pathways, and by increasing the phosphorylation of GluA1 at serine-831 and -845 (*137*). Moreover, tianeptine can regulate the trafficking and synaptic content of both GluA1- and GluA2-containing AMPARs through a CaMKII- and stargazin-dependent mechanism that requires the phosphorylation of stargazin and the interaction of the AMPAR/stargazin complex with PDZ scaffold proteins such as PSD95 (*115*). At the molecular level, phosphorylation of stargazin promotes the stargazin/PSD95 interaction, which in turn recruits and immobilizes AMPARs at post-synaptic sites (*138*).

We found that tianeptine treatment rescued GluA2 expression in Cdkl5-silenced neurons. Despite the molecular mechanisms are still unknown, we hypothesize that this increase may rely on an increased synaptic retention of GluA2-containing AMPARs, leading to decreased internalization and degradation. This model is in agreement with the concomitant decrease of S880 phosphorylation. Further analyses will be aimed to investigate the subunit composition of membrane-inserted AMPARs in tianeptine-treated Cdkl5-silenced neurons.

Of interest, Chu and colleagues showed that tianeptine also exerts neurotrophic effects by promoting neurite outgrowth and synapse formation, as well as synapse homeostasis in hippocampal neurons (*139*). These results were supported by a proteomic analysis, which identified several differentially expressed proteins involved in neurite growth, synaptogenesis and synaptic homeostasis. Among them, tianeptine treatment induced the downregulation of BCBP and ADIP, which are negative regulators of synapse formation, and calpain. Interestingly, calpain is a Ca^{2+}-activated proteinase, that once activated by elevated calcium influx, causes the degradation of many synaptic proteins and contributes to the pathophysiology of various neurological disorders (*140*, *141*). The tianeptine-induced downregulation of calpain may therefore protect neurons from Ca^{2+} overloading.

Overall, these data suggest that besides rescuing GluA2-subunit expression and phosphorylation in Cdkl5-silenced culture, tianeptine treatment may exert therapeutic

effects on spine abnormalities and contribute by regulating Ca^{2+} homeostasis. Based on our results, we find it important with future studies to test the therapeutic potential of tianeptine in preclinical studies of *Cdkl5*-null mice.

4.4 Conclusions

In this dissertation we proposed CDKL5 as a novel regulator of AMPAR composition and trafficking. Our results showed that the impaired expression of GluA2 containing AMPARs can be involved in the synaptic alterations and cognitive deficits associated with CDKL5 disorder. Further analysis will be required to better characterize the involvement of CDKL5 in the molecular complex that coordinates the endosomal sorting of AMPARs towards the plasma membrane, paving the way for new target directed therapeutic approaches. With this aim, we have already identified tianeptine as a promising drug for the treatment of CDKL5-associated AMPAR defects.

5. EXPERIMENTAL PROCEDURES

Antibodies — The following antibodies were used:

Antibody	Code and Supplier	WB	IF: surface	IF: total
CDKL5 *Rabbit polyclonal*	HPA002847 *Sigma-Aldrich*	1:1,000		1:100
CDKL5 *Mouse monoclonal*	sc-376314 *Santa Cruz Biotech.*	1:1,000		1:100
GluR1 *Rabbit polyclonal*	ab86141 *Abcam*	1:1,000		
GluR1 *Rabbit polyclonal*	PC246 *Calbiochem*		1:100	1:100
GluR2 *Mouse monoclonal*	MAB397 *Millipore*	1:1,000	1:200	1:100
LAMP-1 *Rabbit polyclonal*	sc-5570 *Santa Cruz Biotech.*			1:50
GRASP-1 *Rabbit polyclonal*	GTX122295 *GeneTex*	1:500		
MAP2 *Mouse monoclonal*	ab11267 Abcam			1:500
MAP2 *Rabbit polyclonal*	ab32454 Abcam			1:1,000
Class III-β-tubulin (Tuj1) *mouse monoclonal*	MMS-435P Covance	1:10,000		
GAPDH *Rabbit polyclonal*	G9545 *Sigma-Aldrich*	1:10,000		
α-Tubulin *Mouse polyclonal*	*T6074* *Sigma-Aldrich*	1:50,000		
GFP *Chicken polyclonal*	AB16901 *Millipore*			1:100
GFP *Mouse polyclonal*	11814460001 *ROCHE*	1:1,000		

HRP-conjugated goat anti-mouse and -rabbit secondary antibodies for Western blotting were from Thermo Scientific. Secondary Alexa Fluor anti-rabbit, -mouse and -chicken antibodies for immunofluorescence experiments were from Invitrogen.

Plasmids and constructs — pCMV-Flag2B-CDKL5, expressing the human CDKL5_1 isoform has been described elsewhere (*142*). pCMV-Flag2B-CDKL5 (A40V; C152F; Δ781) pathological derivatives were generated by site-directed mutagenesis using the QuickChange site-directed mutagenesis kit (Stratagene). pcDNA3-GFP-GluA1/2 constructs were kindly provided by Prof. Richard L. Huganir. pGW1-GFP-GRASP-1 construct was kindly provided by Prof. Casper C. Hoogenraad. Lentiviral vectors to silence endogenous CDKL5 were generated by cloning double stranded oligonucleotides into the HpaI and XhoI sites of pLentiLox 3.7 (pLL 3.7). The target sequences of the shRNAs are as follows: shCDKL5#1: CTATGGAGTTGTACTTAA; shCDKL5#2: GTGAGAGCGAAAGGCCTT. As control, a shLacZ construct, directed against β-galactosidase, was used. All PCR derived constructs were sequence verified.

Cell cultures and transfections — COS7 and HEK293T cells were maintained in DMEM [Dulbecco's Modified Eagle Medium supplemented with 10% Fetal Bovine Serum, 2 mM L-Glutamine, 100 units/ml penicillin and 100 μg/ml streptomycin (Sigma-Aldrich)] at 37°C with 5% CO_2 in a humidified incubator. Cells were seeded at a density of 7,000 cells/cm^2 or 100,000 cells/ cm^2 respectively for immunofluorescence studies or immunoprecipitations. Transfections were performed 24 h after plating by using Lipofectamine 3000 (Invitrogen) according to manufacturer's instructions. Cells were fixed or harvested 24 h after transfection.

Mice — CD1 and C57BL/6 mice were housed and treated according to the regulations of mouse welfare and ethics and with the approval of the institutional animal care and use committee of the University of Insubria.

Preparation of primary hippocampal cultures — Primary hippocampal cultures were prepared from brains of CD1 mouse embryos at 17 days (E17), considering the day of the

vaginal plug as embryonic day 0. The mice were sacrificed by cervical dislocation, then embryos were recovered and the hippocampi were rapidly dissected. After washing in HBSS (Gibco), the hippocampi were dissociated by 15' incubation at 37°C in 0.25% trypsin (Sigma Aldrich). The cells were suspended in Dissection Medium [Dulbecco's Modified Eagle Medium (DMEM) (Sigma-Aldrich), 10% horse serum (Euroclone), 2 mM L-Glutamine (Sigma), 1 mM Sodium Pyruvate (Gibco)] to block the action of the trypsin. Finally, the cells were plated on poly-L-lysine hydrobromide coated dishes (0.1 mg/ml) or glass coverslips (1 mg/ml) at high density (42,000 cells/cm^2) in Neurobasal Medium [Neurobasal Medium supplemented with B27 (Gibco) and 2 mM L-Glutamine]. After 4 days in vitro (DIV4), cytosine-1-β-D-arabinofuranoside (Sigma-Aldrich) was added to cultured neurons at final concentration of 2 μM to prevent astroglial proliferation. Primary hippocampal neurons were maintained in a humidified incubator with 5% of CO_2 at 37°C.

Cdkl5 silencing —Recombinant lentiviruses were produced by cotransfecting HEK293T cells, grown in 150 mm dishes, with the packaging vectors pVSV-G, pMDL, pREV and either pLL3.7-shCDKL5#1, pLL3.7-shCDKL5#2, or pLL3.7-shLacZ using calcium phosphate. The viral particles were harvested 36 h post-transfection and concentrated by ultracentrifugation with SW32 rotor (Beckman Instruments) at 20,000 rpm for 2 h. Viruses were resuspended in PBS and stored at -80°C. Cultured hippocampal neurons were infected at DIV0, 2 h after plating.

Western blotting (WB) — Western blotting was performed using standard methods. Samples in Laemmli Buffer were separated by 8-10% SDS-PAGE [Acrylamide/Bis-acrylamide solution 37.5:1 (Euro-Clone)], transferred to nitrocellulose membranes and blocked in 5% skimmed milk in Tris-Buffered Saline-Tween-20 (TBS-T): 20 mM Tris-HCl pH 7.5, 150 mM NaCl, supplemented with 0.2% Tween-20 (Sigma-Aldrich). Blots were incubated with primary antibodies in Blocking Solution overnight at 4°C, then washed in in TBS-T and incubated with horseradish-conjugated secondary antibodies in Blocking Solution. After extensive wash, blots were developed with chemiluminescence-based detection system (StoS PSD, Genespin) coupled to G:BOX Chemi Imaging System (Syngene). Densitometric expression analysis were performed using ImageJ software. Phosphorylations were

evaluated as the ratio between phospho-proteins and their non-phosphorylated total isoforms.

Gene expression analysis — Total RNA from hippocampal neurons was isolated using TRIzol Reagent (Invitrogen) according to manufacturer's instructions. Purified RNA was quantified by fluorometric assays with Qubit (Quant-iT RNA HS Reagent, Molecular Probes). To asses RNA quality, 300 ng of sample were resuspended in denaturing RNA Sample Buffer (20% loading dye, 20% formamide) and incubated at 60°C for 10', thereafter RNA was separated through 1% agarose gel electrophoresis. cDNA was synthetized from 500 ng of RNA using iScript Select cDNA Synthesis Kit (Bio-Rad) as indicated by manufacturers. Quantitative Real-Time PCR was performed by using 1/20th of volume of revers transcription reaction and SYBR Select Master Mix (Applied Biosystems) with a real-time cycler BioRad/MJ Research Chromo4. Each sample was assayed in triplicate. The data were analyzed using the ΔΔCt method. A melting curve was automatically generated for each sample and confirmed that a single amplicon was generated in each reaction.
The following primers were used:

Gene ID	Foward sense primer	Reverse antisense primer
Cdkl5	TTCCCAGCTGTTAACCATCC	AAGGAGACCGGTCCAAAAGT
GluA2	AAGGAGGAAAGGGAAACGAG	CCGAAGTGGAAAACTGAACC
Gapdh	ATTGTCAGCAATGCATCCTG	ATGGACTGTGGTCATGAGCC

Immunofluorescence (IF) — Primary hippocampal neurons plated on glass coverslips were fixed at DIV 18 with 4% paraformaldehyde/PBS for 15 minutes and incubated with Blocking Solution (5% horse serum in PBS in the presence or absence of 0.2% Triton X-100) for 1h at room temperature, and then with primary antibodies overnight at 4°C in blocking solution. Primary antibody raised against extracellular epitopes of GluA1-GluA2 were used for the surface–expressed AMPARs. The addition of 0.2% Triton X-100 was omitted for the detection of surface-expressed receptor proteins. After washing in PBS, the neurons were incubated with secondary antibodies (Molecular Probes) for 1 h at room temperature. Coverslips were

mounted for microscopy using ProLong Gold antifade reagent (Molecular Probes). GluA1 and GluA2 immunofluorescence intensities were analysed on a fixed region of $MAP2^+$ dendritic branches of GFP positive neurons. The surface-to-total ratio was calculated as the ratio between surface and total GluA1-GluA2 fluorescence intensities from neurons grown on different glass coverslips but belonging to the same experiment.

Spine morphology and number were analysed on $MAP2^+$ dendritic branches of neurons at DIV18 using GFP expression to highlight the neuronal structure.

COS-7 cells grown on glass coverslips were fixed 24h after transfection and processed similarly to hippocampal neurons for surface and total AMPAR-staining. The surface-to-total ratio was calculated as the ratio between surface and total GluA1-GluA2 fluorescence intensities from single cell area.

Images were captured using a x60 or x100-oil immersion objective coupled to an Olympus BX51 Fluorescence microscope equipped with Retiga R1 (QImaging) CCD camera. Fluorescence quantifications were performed with Image J software.

Antibody feeding — The current fluorescence-based antibody feeding assay was adapted from Hoogenraad et al. (*124*). Primary hippocampal neurons (DIV 17) were *live* labelled for GluA2 subunits with a mouse monoclonal antibody against an extracellular epitope at a concentration of 10 µg/ml by incubating coverslips in conditioned medium for 10 min at 37°C. After a brief wash in prewarmed DMEM, neurons were alternatively fixed for surface staining or processed for subsequent stimulation. To induce AMPAR internalization, cultures were either stimulated for 2 min with 100 µM AMPA + 50 µM APV (selective NMDA receptor antagonist) or vehicle, as control, then returned to conditioned medium and incubated for 30 min. The remaining surface anti-GluA2 antibody was stripped away by incubation in stripping buffer (0.5 M NaCl/ 0.2 M acetic acid in PBS) on ice for 4 min and washed extensively with ice-cold PBS. Finally, neurons were fixed with 4% paraformaldehyde/PBS for 15' at room temperature. Surface or internalized GluA2-subunits were detected with anti-mouse fluorescent secondary antibodies. Coverslips were pre-incubated with LAMP-1 antibody overnight at 4°C for the co-localization with internalized GluA2.

Cell-surface protein biotinylation — Primary hippocampal neurons (DIV 18) were washed with HBSS-glucose (HBSS supplemented with 1% glucose) and then incubated with EZ-link sulfo-NHS-SS-Biotin (0,75 mg/ml in HBSS-glucose) for 25 min at 4°C to prevent receptor internalization. Unreacted biotin was quenched with Quenching Solution (1% BSA in HBSS-glucose) for 10 min at 4°C. After washing, hippocampal neurons were lysed in RIPA Buffer (50 mM Tris-HCl pH 8, 150 mM NaCl, 1mM EDTA, 1% di Triton X-100, 1% sodium deoxycholate, 0,1% SDS and supplemented with PIC) for 1 h at 4°C on a rotating wheel. Lysates were clarified by centrifugation at 16000 g for 15 min at 4°C and the supernatants were collected and quantified with BCA assay (Thermo Scientific). 200 μg of protein extract were incubated with UltraLink Streptavidin beads (Thermo Scientific) in RIPA Buffer on rotating wheel for 2 h at 4°C. Cell-surface biotinylated proteins were pulled-down by centrifugation, washed in RIPA Buffer and analysed by Western blotting.

Calcium Imaging — Primary hippocampal neurons at DIV 16 were loaded with calcium-sensitive dye by incubation in 10 μM of Rhod-3 (Molecular Probes) in KRH (Krebs'–Ringer's–HEPES) (125 mM NaCl, 5 mM KCl, 1.2 mM MgSO4, 1.2 mM KH_2PO_4, 25 mM HEPES, 6 mM glucose, 2 mM CaCl2, pH 7.4) according to manufacturer's instructions. To prevent calcium influx from NMDARs the extracellular solution was supplemented with 100 μM of the NMDAR antagonist APV. After rinses in KRH, coverslips were mounted in recording chambers that were placed on the stage of an UltraVIEW ERS Spinning Disk Confocal microscope (PerkinElmer). Images were captured using a x40 oil immersion objective. Time-lapse recording of calcium dynamics was performed with fixed exposure time and excitation intensity with an acquisition rate of 1 Hz for 60 sec. Calcium dynamics were measured with Image J software selecting Regions Of interest (ROIs) that were drawn on the cell cytoplasm.

Pharmacological treatments — Primary hippocampal neurons were treated at DIV11 with Tianeptine in conditioned medium at the final concentration of 10 μM and replenished every second day (DIV13, DIV15, DIV17) till DIV18 when neurons were harvested for Western blotting analysis.

Yeast two-hybrid screening — The yeast two-hybrid (Y2H) screening was performed by Hybrigenics Services, S.A.S, Paris, France (http://www.hybrigenics-services.com). The C-terminus of human CDKL5 (amino acids 299–1030; GenBank accession number gi: 83367068) fused to the Gal4 DNA-binding domain and expressed from the inducible pB35 vector, was used as bait to screen a random-primed Human Adult Brain cDNA library constructed into pP6. 113 million clones (11-fold the complexity of the library) were screened using a mating approach with Y187 (MATα Gal4Δ Gal80Δ ade2-101 his3 leu2-3,-112 trp1-901 ura3-52 URA3::UASGAL1-LacZ, (met-)) and CG1945 (MATa Gal4-452 Gal80-538 ade2-101 his3-D200 leu2-3,112 trp1-901 ura3-52 lys2-801 URA3::Gal4 17mers (X3)-CyC1TATA-LacZ lys2::GAL1UAS-GAL1TATA-HIS3 cyhR) yeast strains. A total of 171 His+ colonies were selected on a medium lacking tryptophan, leucine, methionine and histidine. The prey fragments of the positive clones were amplified by PCR and sequenced at their 5' and 3' junctions. The resulting sequences were used to identify the corresponding interacting proteins in the GenBank database (NCBI) using a fully automated procedure. A confidence score (PBS, for Predicted Biological Score) was attributed to each interaction as previously described (*143*).

Immunoprecipitation (IP) — HEK293T and mouse brains were lysed on ice for 30 min with Lysis Buffer: Lysis Buffer: 50 mM Tris-HCl pH 7.4, 150 mM NaCl, 1 mM EDTA, 1 mM EGTA, 1% Triton X-100, supplemented with protease inhibitor (PIC, Sigma-Aldrich) and phosphatase inhibitor (PhosStop, Roche) cocktails. Lysates were clarified by centrifugation at 16000 g for 15 min at 4°C and the supernatants were collected and quantified with Bradford assay (Bio-Rad). Exogenously expressed GPF-GRASP was immunoprecipitated from 400 µg of HEK293T cell extract with 0,6 µg of anti-GFP antibody. For *in vivo* immunoprecipitations, 1 mg of brain extract was incubated with 1 µg of anti-CDKL5 antibody, or unrelated IgGs as control. Lysates were incubated on rotating wheel overnight at 4°C. The immunocomplexes were immunoprecipitated with Protein G Agarose (Invitrogen), then washed in Lysis Buffer and analysed by Western blotting.

Two-Dimensional Isoelectric Focusing — Brains from post-natal day 5 and 25 (P5 and P25) were isolated and lysed in UTC buffer (7 M urea, 2 M thiourea, 4% CHAPS).

Approximately 200 µg of extract were loaded on 7 cm IPG DryStrips with a linear 4–7 pH gradient and isoelectric focusing performed with an IPGphor II apparatus (GE Healthcare) according to the manufacturer's instructions. Subsequent SDS-PAGE was performed using 8% gels and proteins were detected by Western blotting. Phosphatase treatment was done by adding 100 units of Lambda Protein Phosphatase (λPP; New England Biolabs) to the extract diluted in 2 ml 0.1% SDS, 0.1 mM MnCl2, and 1x phosphatase-buffer. After an overnight incubation at 30°C the samples were concentrated with Ultracel 10K centrifugal filters (Millipore) and subjected to isoelectric focusing.

Statistical Analysis — All values are expressed as the mean±SEM. The significance of results was evaluated by Student's t test, one-way ANOVA followed by Dunnett's or Tuckey's multiple comparison test when appropriate.

Nomenclature - CDKL5 written in upper case letters refers to the human protein, whereas Cdkl5 in lower case letters refers to the murine counterpart. *CDKL5* and *Cdkl5* reported in *italics* indicate, alternatively, the human and the murine genes and transcripts.

6. ACKNOWLEDGEMENTS

Firstly, I would like to express my sincere gratitude to my supervisor **Prof. Charlotte Kilstrup-Nielsen** for the continuous support of my Ph.D study and related research, for her patience and encouragement. Her guidance helped me throughout the difficulties of my research and in writing of this thesis.

Thanks to **Prof. Nicoletta Landberger** for her precious advices.

A special thank goes to **Laura Rusconi** for her insightful comments and for the hard questions which stimulated me to widen my research from various perspectives. Her extensive knowledge and experience guided me, and without her precious support it would not be possible to conduct this research.

I would like to thank my former and present colleagues: **Anna Bergo**, **Maria Maddalena Valente**, **Paolo La Montanara**, **Paolo Motta**, **Barbara Leva**, **Maria Fazzari** and **Diana Peroni**. Thanks for the stimulating discussions and for all the fun we have had in the last three years.
A special thank goes to **Isabella Barbiero** for sharing with me ups and downs, the laughter and for the continuous support.

Thanks to **my family** and, in particular, to my mum **Giovanna**: who I am and all the results I have achieved were because of her.

Last but foremost, thanks to **Marta** for sharing her life with me and for giving me all the strength and the support. She believes in me as I do.

7. REFERENCES

1. E. Montini *et al.*, Identification and Characterization of a Novel Serine– Threonine Kinase Gene from the Xp22 Region. *Genomics*. **51**, 427–433 (1998).
2. V. M. Kalscheuer *et al.*, Disruption of the Serine/Threonine Kinase 9 Gene Causes Severe X-Linked Infantile Spasms and Mental Retardation. *Am. J. Hum. Genet.* **72**, 1401–1411 (2003).
3. L. S. Weaving *et al.*, Mutations of CDKL5 cause a severe neurodevelopmental disorder with infantile spasms and mental retardation. *Am. J. Hum. Genet.* **75**, 1079–93 (2004).
4. J. Tao *et al.*, Mutations in the X-linked cyclin-dependent kinase-like 5 (CDKL5/STK9) gene are associated with severe neurodevelopmental retardation. *Am. J. Hum. Genet.* **75**, 1149–54 (2004).
5. F. Hanefeld, The clinical pattern of the Rett syndrome. *Brain Dev.* **7**, 320–5 (1985).
6. J. C. Beal, K. Cherian, S. L. Moshe, Early-Onset Epileptic Encephalopathies: Ohtahara Syndrome and Early Myoclonic Encephalopathy. *Pediatr. Neurol.* **47**, 317–323 (2012).
7. G. M. Mirzaa *et al.*, CDKL5 and ARX mutations in males with early-onset epilepsy. *Pediatr. Neurol.* **48**, 367–77 (2013).
8. S. Fehr *et al.*, The CDKL5 disorder is an independent clinical entity associated with early-onset encephalopathy. *Eur. J. Hum. Genet.* **21**, 266–273 (2012).
9. S. Fehr *et al.*, Functional abilities in children and adults with the CDKL5 disorder. *Am. J. Med. Genet. Part A*. **5** (2016), doi:10.1002/ajmg.a.37851.
10. L. S. Weaving *et al.*, Mutations of CDKL5 cause a severe neurodevelopmental disorder with infantile spasms and mental retardation. *Am. J. Hum. Genet.* **75**, 1079–93 (2004).
11. G. Pini *et al.*, Variant of Rett Syndrome and CDKL5 Gene: Clinical and Autonomic Description of 10 Cases. *Neuropediatrics*. **43**, 037–043 (2012).
12. R. D. Hector *et al.*, Characterisation of CDKL5 Transcript Isoforms in Human and Mouse. *PLoS One*. **11**, e0157758 (2016).
13. S. L. Williamson *et al.*, A novel transcript of cyclin-dependent kinase-like 5 (CDKL5) has an alternative C-terminus and is the predominant transcript in brain. *Hum. Genet.* **131**, 187–200 (2012).
14. C. Kilstrup-Nielsen *et al.*, What we know and would like to know about CDKL5 and its involvement in epileptic encephalopathy. *Neural Plast.* **2012**, 728267 (2012).
15. P. La Montanara *et al.*, Synaptic synthesis, dephosphorylation, and degradation: a

novel paradigm for an activity-dependent neuronal control of CDKL5. *J. Biol. Chem.* **290**, 4512–27 (2015).

16. I. Bertani *et al.*, Functional consequences of mutations in CDKL5, an X-linked gene involved in infantile spasms and mental retardation. *J. Biol. Chem.* **281**, 32048–56 (2006).

17. L. Rusconi, C. Kilstrup-Nielsen, N. Landsberger, Extrasynaptic N-Methyl-D-aspartate (NMDA) receptor stimulation induces cytoplasmic translocation of the CDKL5 kinase and its proteasomal degradation. *J. Biol. Chem.* **286**, 36550–36558 (2011).

18. L. Rusconi *et al.*, C1. L. Rusconi et al., CDKL5 Expression Is Modulated during Neuronal Development and Its Subcellular Distribution Is Tightly Regulated by the C-terminal Tail. J. Biol. Chem. 283, 30101–30111 (2008).DKL5 Expression Is Modulated during Neuronal Development . *J. Biol. Chem.* **283**, 30101–30111 (2008).

19. J. Mertz *et al.*, Sequential Elution Interactome Analysis of the Mind Bomb 1 Ubiquitin Ligase Reveals a Novel Role in Dendritic Spine Outgrowth. *Mol. Cell. Proteomics*. **14**, 1898–910 (2015).

20. E.-A. Choe *et al.*, Neuronal Morphogenesis Is Regulated by the Interplay between Cyclin-Dependent Kinase 5 and the Ubiquitin Ligase Mind Bomb 1. *J. Neurosci.* **27**, 9503–9512 (2007).

21. K.-J. Yoon *et al.*, Mind bomb-1 is an essential modulator of long-term memory and synaptic plasticity via the Notch signaling pathway. *Mol. Brain*. **5**, 40 (2012).

22. J. Christodoulou, A. Grimm, T. Maher, B. Bennetts, RettBASE: The IRSA MECP2 variation database—a new mutation database in evolution. *Hum. Mutat.* **21**, 466–472 (2003).

23. P. Szafranski *et al.*, Neurodevelopmental and neurobehavioral characteristics in males and females with CDKL5 duplications. *Eur. J. Hum. Genet.* **23**, 915–921 (2015).

24. H. Rosas-Vargas *et al.*, Impairment of CDKL5 nuclear localisation as a cause for severe infantile encephalopathy. *J. Med. Genet.* **45**, 172–178 (2007).

25. I. Bertani *et al.*, Functional Consequences of Mutations in CDKL5, an X-linked Gene Involved in Infantile Spasms and Mental Retardation. *J. Biol. Chem.* **281**, 32048–32056 (2006).

26. S. Fehr *et al.*, Functional abilities in children and adults with the CDKL5 disorder. *Am. J. Med. Genet. Part A*. **170**, 2860–2869 (2016).

27. C. Sala, S. Rudolph-Correia, M. Sheng, Developmentally regulated NMDA receptor-dependent dephosphorylation of cAMP response element-binding protein (CREB) in hippocampal neurons. *J. Neurosci.* **20**, 3529–36 (2000).

28. S. Ricciardi *et al.*, CDKL5 ensures excitatory synapse stability by reinforcing NGL-1-PSD95 interaction in the postsynaptic compartment and is impaired in patient iPSC-derived neurons. *Nat. Cell Biol.* **14**, 911–23 (2012).

29. Y.-C. Zhu *et al.*, Palmitoylation-dependent CDKL5-PSD-95 interaction regulates synaptic targeting of CDKL5 and dendritic spine development. *Proc. Natl. Acad. Sci. U. S. A.* **110**, 9118–23 (2013).

30. I.-T. J. Wang *et al.*, Loss of CDKL5 disrupts kinome profile and event-related potentials leading to autistic-like phenotypes in mice. *Proc. Natl. Acad. Sci. U. S. A.* **109**, 21516–21 (2012).

31. E. Amendola *et al.*, Mapping pathological phenotypes in a mouse model of CDKL5 disorder. *PLoS One*. **9**, 5–16 (2014).

32. S. Trazzi *et al.*, *Hum. Mol. Genet.*, in press, doi:10.1093/hmg/ddw231.

33. G. Della Sala *et al.*, Dendritic Spine Instability in a Mouse Model of CDKL5 Disorder Is Rescued by Insulin-like Growth Factor 1. *Biol. Psychiatry*. **80**, 302–311 (2014).

34. T. V Bliss, T. Lomo, Long-lasting potentiation of synaptic transmission in the dentate area of the anaesthetized rabbit following stimulation of the perforant path. *J. Physiol.* **232**, 331–56 (1973).

35. W. Wisden, P. H. Seeburg, Mammalian ionotropic glutamate receptors. *Curr. Opin. Neurobiol.* **3**, 291–8 (1993).

36. C. Rosenmund, Y. Stern-Bach, C. F. Stevens, The tetrameric structure of a glutamate receptor channel. *Science*. **280**, 1596–9 (1998).

37. A. M. Craig, C. D. Blackstone, R. L. Huganir, G. Banker, The distribution of glutamate receptors in cultured rat hippocampal neurons: postsynaptic clustering of AMPA-selective subunits. *Neuron*. **10**, 1055–68 (1993).

38. R. J. Wenthold, R. S. Petralia, I. I. Blahos J, A. S. Niedzielski, Evidence for multiple AMPA receptor complexes in hippocampal CA1/CA2 neurons. *J. Neurosci.* **16**, 1982–9 (1996).

39. J. J. Zhu, J. A. Esteban, Y. Hayashi, R. Malinow, Postnatal synaptic potentiation: delivery of GluR4-containing AMPA receptors by spontaneous activity. *Nat. Neurosci.* **3**, 1098–106 (2000).

40. V. Bernard, P. Somogyi, J. P. Bolam, Cellular, subcellular, and subsynaptic distribution of AMPA-type glutamate receptor subunits in the neostriatum of the rat. *J. Neurosci.* **17**, 819–33 (1997).

41. K. A. Pelkey *et al.*, Pentraxins coordinate excitatory synapse maturation and circuit integration of parvalbumin interneurons. *Neuron*. **85**, 1257–72 (2015).

42. M. Hollmann, S. Heinemann, Cloned glutamate receptors. *Annu. Rev. Neurosci.* **17**, 31–108 (1994).

43. R. Dingledine, K. Borges, D. Bowie, S. F. Traynelis, The glutamate receptor ion channels. *Pharmacol. Rev.* **51**, 7–61 (1999).

44. J. D. Shepherd, R. L. Huganir, The cell biology of synaptic plasticity: AMPA receptor

trafficking. *Annu. Rev. Cell Dev. Biol.* **23**, 613–43 (2007).

45. V. Anggono, R. L. Huganir, Regulation of AMPA receptor trafficking and synaptic plasticity. *Curr. Opin. Neurobiol.* **22**, 461–9 (2012).

46. B. Sommer *et al.*, Flip and flop: a cell-specific functional switch in glutamate-operated channels of the CNS. *Science*. **249**, 1580–5 (1990).

47. J. Mosbacher *et al.*, A molecular determinant for submillisecond desensitization in glutamate receptors. *Science*. **266**, 1059–62 (1994).

48. C. Bellone, R. A. Nicoll, Rapid bidirectional switching of synaptic NMDA receptors. *Neuron*. **55**, 779–85 (2007).

49. I. H. Greger, L. Khatri, X. Kong, E. B. Ziff, AMPA receptor tetramerization is mediated by Q/R editing. *Neuron*. **40**, 763–74 (2003).

50. M. Higuchi *et al.*, Point mutation in an AMPA receptor gene rescues lethality in mice deficient in the RNA-editing enzyme ADAR2. *Nature*. **406**, 78–81 (2000).

51. T. Kuner, C. Beck, B. Sakmann, P. H. Seeburg, Channel-lining residues of the AMPA receptor M2 segment: structural environment of the Q/R site and identification of the selectivity filter. *J. Neurosci.* **21**, 4162–72 (2001).

52. N. P. Whitney *et al.*, Calcium-permeable AMPA receptors containing Q/R-unedited GluR2 direct human neural progenitor cell differentiation to neurons. *FASEB J.* **22**, 2888–900 (2008).

53. J. T. R. Isaac, M. Ashby, C. J. McBain, The Role of the GluR2 Subunit in AMPA Receptor Function and Synaptic Plasticity. *Neuron*. **54**, 859–871 (2007).

54. S. Cull-Candy, L. Kelly, M. Farrant, Regulation of Ca2+-permeable AMPA receptors: synaptic plasticity and beyond. *Curr. Opin. Neurobiol.* **16**, 288–97 (2006).

55. H. Monyer, P. H. Seeburg, W. Wisden, Glutamate-operated channels: developmentally early and mature forms arise by alternative splicing. *Neuron*. **6**, 799–810 (1991).

56. K. M. Partin, D. K. Patneau, M. L. Mayer, Cyclothiazide differentially modulates desensitization of alpha-amino-3-hydroxy-5-methyl-4-isoxazolepropionic acid receptor splice variants. *Mol. Pharmacol.* **46**, 129–38 (1994).

57. R. J. O'Brien *et al.*, Synaptic clustering of AMPA receptors by the extracellular immediate-early gene product Narp. *Neuron*. **23**, 309–23 (1999).

58. D. Xu *et al.*, Narp and NP1 form heterocomplexes that function in developmental and activity-dependent synaptic plasticity. *Neuron*. **39**, 513–28 (2003).

59. L. Saglietti *et al.*, Extracellular interactions between GluR2 and N-cadherin in spine regulation. *Neuron*. **54**, 461–77 (2007).

60. M. Passafaro, T. Nakagawa, C. Sala, M. Sheng, Induction of dendritic spines by an extracellular domain of AMPA receptor subunit GluR2. *Nature*. **424**, 677–681 (2003).

61. A. S. Leonard, M. A. Davare, M. C. Horne, C. C. Garner, J. W. Hell, SAP97 is associated with the alpha-amino-3-hydroxy-5-methylisoxazole-4-propionic acid receptor GluR1 subunit. *J. Biol. Chem.* **273**, 19518–24 (1998).

62. H. K. Lee, M. Barbarosie, K. Kameyama, M. F. Bear, R. L. Huganir, Regulation of distinct AMPA receptor phosphorylation sites during bidirectional synaptic plasticity. *Nature*. **405**, 955–9 (2000).

63. M. Colledge *et al.*, Targeting of PKA to glutamate receptors through a MAGUK-AKAP complex. *Neuron*. **27**, 107–19 (2000).

64. N. Sans *et al.*, Synapse-associated protein 97 selectively associates with a subset of AMPA receptors early in their biosynthetic pathway. *J. Neurosci.* **21**, 7506–16 (2001).

65. H. Dong *et al.*, GRIP: a synaptic PDZ domain-containing protein that interacts with AMPA receptors. *Nature*. **386**, 279–84 (1997).

66. H. Dong, P. Zhang, D. Liao, R. L. Huganir, Characterization, expression, and distribution of GRIP protein. *Ann. N. Y. Acad. Sci.* **868**, 535–40 (1999).

67. S. Srivastava *et al.*, Novel anchorage of GluR2/3 to the postsynaptic density by the AMPA receptor-binding protein ABP. *Neuron*. **21**, 581–91 (1998).

68. L. Shen, F. Liang, L. D. Walensky, R. L. Huganir, Regulation of AMPA receptor GluR1 subunit surface expression by a 4. 1N-linked actin cytoskeletal association. *J. Neurosci.* **20**, 7932–40 (2000).

69. A. Nishimune *et al.*, NSF binding to GluR2 regulates synaptic transmission. *Neuron*. **21**, 87–97 (1998).

70. S. H. Lee, L. Liu, Y. T. Wang, M. Sheng, Clathrin adaptor AP2 and NSF interact with overlapping sites of GluR2 and play distinct roles in AMPA receptor trafficking and hippocampal LTD. *Neuron*. **36**, 661–74 (2002).

71. A. C. Jackson, R. A. Nicoll, The Expanding Social Network of Ionotropic Glutamate Receptors: TARPs and Other Transmembrane Auxiliary Subunits. *Neuron*. **70**, 178–199 (2011).

72. E. Díaz, Regulation of AMPA receptors by transmembrane accessory proteins. *Eur. J. Neurosci.* **32**, 261–268 (2010).

73. S. Tomita, Regulation of Ionotropic Glutamate Receptors by Their Auxiliary Subunits. *Physiology*. **25** (2010).

74. A. C. Jackson *et al.*, Probing TARP modulation of AMPA receptor conductance with polyamine toxins. *J. Neurosci.* **31**, 7511–20 (2011).

75. M. L. Mayer, Glutamate receptors at atomic resolution. *Nature*. **440**, 456–62 (2006).

76. M. Sukumaran, A. C. Penn, I. H. Greger, AMPA receptor assembly: atomic determinants and built-in modulators. *Adv. Exp. Med. Biol.* **970**, 241–64 (2012).

77. M. Rossmann *et al.*, Subunit-selective N-terminal domain associations organize the

formation of AMPA receptor heteromers. *EMBO J.* **30**, 959–71 (2011).

78. T. Nakagawa, The Biochemistry, Ultrastructure, and Subunit Assembly Mechanism of AMPA Receptors. *Mol. Neurobiol.* **42**, 161–184 (2010).

79. S. J. Mah, E. Cornell, N. A. Mitchell, M. W. Fleck, Glutamate receptor trafficking: endoplasmic reticulum quality control involves ligand binding and receptor function. *J. Neurosci.* **25**, 2215–25 (2005).

80. W. Lu, L. Khatri, E. B. Ziff, Trafficking of ??-amino-3-hydroxy-5-methyl-4-isoxazolepropionic acid receptor (AMPA) receptor subunit GluA2 from the endoplasmic reticulum is stimulated by a complex containing Ca2+/calmodulin-activated kinase II (CaMKII) and PICK1 protein and by release . *J. Biol. Chem.* **289**, 19218–19230 (2014).

81. N. Sans *et al.*, Synapse-associated protein 97 selectively associates with a subset of AMPA receptors early in their biosynthetic pathway. *J. Neurosci.* **21**, 7506–16 (2001).

82. A. C. Horton, M. D. Ehlers, Secretory trafficking in neuronal dendrites. *Nat. Cell Biol.* **6**, 585–91 (2004).

83. K. Huang, A. El-Husseini, Modulation of neuronal protein trafficking and function by palmitoylation. *Curr. Opin. Neurobiol.* **15**, 527–35 (2005).

84. A. E.-D. El-Husseini *et al.*, Synaptic strength regulated by palmitate cycling on PSD-95. *Cell*. **108**, 849–63 (2002).

85. M. Yamazaki *et al.*, Differential palmitoylation of two mouse glutamate receptor interacting protein 1 forms with different N-terminal sequences. *Neurosci. Lett.* **304**, 81–4 (2001).

86. S. DeSouza, J. Fu, B. A. States, E. B. Ziff, Differential palmitoylation directs the AMPA receptor-binding protein ABP to spines or to intracellular clusters. *J. Neurosci.* **22**, 3493–503 (2002).

87. T. Hayashi, G. Rumbaugh, R. L. Huganir, Differential regulation of AMPA receptor subunit trafficking by palmitoylation of two distinct sites. *Neuron*. **47**, 709–23 (2005).

88. N. Hirokawa, R. Takemura, Molecular motors and mechanisms of directional transport in neurons. *Nat. Rev. Neurosci.* **6**, 201–14 (2005).

89. M. Setou *et al.*, Glutamate-receptor-interacting protein GRIP1 directly steers kinesin to dendrites. *Nature*. **417**, 83–87 (2002).

90. M. Wyszynski *et al.*, Interaction between GRIP and liprin-alpha/SYD2 is required for AMPA receptor targeting. *Neuron*. **34**, 39–52 (2002).

91. S. Y. Grooms *et al.*, Activity bidirectionally regulates AMPA receptor mRNA abundance in dendrites of hippocampal neurons. *J. Neurosci.* **26**, 8339–51 (2006).

92. R. C. Malenka, M. F. Bear, LTP and LTD: an embarrassment of riches. *Neuron*. **44**, 5–21 (2004).

93. R. C. Malenka, R. A. Nicoll, NMDA-receptor-dependent synaptic plasticity: multiple forms and mechanisms. *Trends Neurosci.* **16**, 521–7 (1993).

94. Y. Yang, X.-B. Wang, Q. Zhou, Perisynaptic GluR2-lacking AMPA receptors control the reversibility of synaptic and spines modifications. *Proc. Natl. Acad. Sci. U. S. A.* **107**, 11999–2004 (2010).

95. N. Jaafari, J. M. Henley, J. G. Hanley, PICK1 mediates transient synaptic expression of GluA2-lacking AMPA receptors during glycine-induced AMPA receptor trafficking. *J. Neurosci.* **32**, 11618–30 (2012).

96. K. He *et al.*, Stabilization of Ca2+-permeable AMPA receptors at perisynaptic sites by GluR1-S845 phosphorylation. *Proc. Natl. Acad. Sci. U. S. A.* **106**, 20033–8 (2009).

97. S. Bassani, A. Folci, J. Zapata, M. Passafaro, AMPAR trafficking in synapse maturation and plasticity. *Cell. Mol. Life Sci.* **70**, 4411–30 (2013).

98. H. Adesnik, R. A. Nicoll, Conservation of Glutamate Receptor 2-Containing AMPA Receptors during Long-Term Potentiation. *J. Neurosci.* **27** (2007).

99. E. E. Gray, A. E. Fink, J. Sariñana, B. Vissel, T. J. O'Dell, Long-term potentiation in the hippocampal CA1 region does not require insertion and activation of GluR2-lacking AMPA receptors. *J. Neurophysiol.* **98**, 2488–92 (2007).

100. K. K. Dev, A. Nishimune, J. M. Henley, S. Nakanishi, The protein kinase C alpha binding protein PICK1 interacts with short but not long form alternative splice variants of AMPA receptor subunits. *Neuropharmacology*. **38**, 635–44 (1999).

101. J. L. Perez *et al.*, PICK1 targets activated protein kinase Calpha to AMPA receptor clusters in spines of hippocampal neurons and reduces surface levels of the AMPA-type glutamate receptor subunit 2. *J. Neurosci.* **21**, 5417–28 (2001).

102. S. Matsuda, S. Mikawa, H. Hirai, Phosphorylation of serine-880 in GluR2 by protein kinase C prevents its C terminus from binding with glutamate receptor-interacting protein. *J. Neurochem.* **73**, 1765–8 (1999).

103. H. J. Chung, J. Xia, R. H. Scannevin, X. Zhang, R. L. Huganir, Phosphorylation of the AMPA receptor subunit GluR2 differentially regulates its interaction with PDZ domain-containing proteins. *J. Neurosci.* **20**, 7258–67 (2000).

104. C. H. Kim, H. J. Chung, H. K. Lee, R. L. Huganir, Interaction of the AMPA receptor subunit GluR2/3 with PDZ domains regulates hippocampal long-term depression. *Proc. Natl. Acad. Sci. U. S. A.* **98**, 11725–30 (2001).

105. Y. Wu *et al.*, Mutations in ionotropic AMPA receptor 3 alter channel properties and are associated with moderate cognitive impairment in humans.

106. W.-Q. Zhao *et al.*, Inhibition of Calcineurin-mediated Endocytosis and -Amino-3-hydroxy-5-methyl-4-isoxazolepropionic Acid (AMPA) Receptors Prevents Amyloid Oligomer-induced Synaptic Disruption. *J. Biol. Chem.* **285**, 7619–7632 (2010).

107. D. J. Whitcomb *et al.*, Intracellular oligomeric amyloid-beta rapidly regulates GluA1 subunit of AMPA receptor in the hippocampus. *Sci. Rep.* **5**, 10934 (2015).

108. J. M. Spaethling, D. M. Klein, P. Singh, D. F. Meaney, Calcium-permeable AMPA receptors appear in cortical neurons after traumatic mechanical injury and contribute to neuronal fate. *J. Neurotrauma*. **25**, 1207–16 (2008).

109. S. Y. Grooms, T. Opitz, M. V Bennett, R. S. Zukin, Status epilepticus decreases glutamate receptor 2 mRNA and protein expression in hippocampal pyramidal cells before neuronal death. *Proc. Natl. Acad. Sci. U. S. A.* **97**, 3631–6 (2000).

110. M. L. Mignogna *et al.*, The intellectual disability protein RAB39B selectively regulates GluA2 trafficking to determine synaptic AMPAR composition. *Nat. Commun.* **6**, 6504 (2015).

111. W. Li, X. Xu, L. Pozzo-Miller, Excitatory synapses are stronger in the hippocampus of Rett syndrome mice due to altered synaptic trafficking of AMPA-type glutamate receptors. *Proc. Natl. Acad. Sci.* **113**, E1575–E1584 (2016).

112. P. V Hornbeck *et al.*, PhosphoSitePlus, 2014: mutations, PTMs and recalibrations. *Nucleic Acids Res.* **43** (2015), doi:10.1093/nar/gku1267.

113. A. Meneses, Tianeptine: 5-HT uptake sites and 5-HT(1-7) receptors modulate memory formation in an autoshaping Pavlovian/instrumental task. *Neurosci. Biobehav. Rev.* **26**, 309–19 (2002).

114. R. Jaffard *et al.*, Effects of tianeptine on spontaneous alternation, simple and concurrent spatial discrimination learning and on alcohol-induced alternation deficits in mice. *Behav. Pharmacol.* **2**, 37–46 (1991).

115. H. Zhang *et al.*, Regulation of AMPA receptor surface trafficking and synaptic plasticity by a cognitive enhancer and antidepressant molecule. *Mol. Psychiatry*. **18**, 471–84 (2013).

116. S.-H. Shi, Y. Hayashi, J. A. Esteban, R. Malinow, Subunit-Specific Rules Governing AMPA Receptor Trafficking to Synapses in Hippocampal Pyramidal Neurons. *Cell*. **105**, 331–343 (2001).

117. H. J. Chung, J. Xia, R. H. Scannevin, X. Zhang, R. L. Huganir, Phosphorylation of the AMPA Receptor Subunit GluR2 Differentially Regulates Its Interaction with PDZ Domain-Containing Proteins. *J. Neurosci.* **20** (2000).

118. R. C. Evans, K. T. Blackwell, Calcium: amplitude, duration, or location? *Biol. Bull.* **228**, 75–83 (2015).

119. M. Giannandrea *et al.*, Mutations in the small GTPase gene RAB39B are responsible for X-linked mental retardation associated with autism, epilepsy, and macrocephaly. *Am. J. Hum. Genet.* **86**, 185–95 (2010).

120. Z. Qiu *et al.*, The Rett Syndrome Protein MeCP2 Regulates Synaptic Scaling, doi:10.1523/JNEUROSCI.0175-11.2012.

121. M. V. C. Nguyen *et al.*, MeCP2 is critical for maintaining mature neuronal networks and global brain anatomy during late stages of postnatal brain development and in the mature adult brain. *J. Neurosci.* **32**, 10021–34 (2012).

122. I. Bertani *et al.*, Functional Consequences of Mutations in CDKL5, an X-linked Gene Involved in Infantile Spasms and Mental Retardation * (2006), doi:10.1074/jbc.M606325200.

123. B. Ye *et al.*, GRASP-1: A Neuronal RasGEF Associated with the AMPA Receptor/GRIP Complex. *Neuron*. **26**, 603–617 (2000).

124. C. C. Hoogenraad *et al.*, Neuron specific Rab4 effector GRASP-1 coordinates membrane specialization and maturation of recycling endosomes. *PLoS Biol.* **8**, e1000283 (2010).

125. M. Park, E. C. Penick, J. G. Edwards, J. A. Kauer, M. D. Ehlers, Recycling Endosomes Supply AMPA Receptors for LTP. *Science (80-.).* **305**, 1972–1975 (2004).

126. T. C. Brown, S. S. Correia, C. N. Petrok, J. A. Esteban, Functional Compartmentalization of Endosomal Trafficking for the Synaptic Delivery of AMPA Receptors during Long-Term Potentiation, doi:10.1523/JNEUROSCI.4258-07.2007.

127. B. Sönnichsen, S. De Renzis, E. Nielsen, J. Rietdorf, M. Zerial, Distinct membrane domains on endosomes in the recycling pathway visualized by multicolor imaging of Rab4, Rab5, and Rab11. *J. Cell Biol.* **149**, 901–14 (2000).

128. T. S. Niranjan *et al.*, Affected Kindred Analysis of Human X Chromosome Exomes to Identify Novel X-Linked Intellectual Disability Genes. *PLoS One*. **10** (2015), doi:10.1371/journal.pone.0116454.

129. B. H. Y. Chung *et al.*, Phenotypic spectrum associated with duplication of Xp11.22-p11.23 includes Autism Spectrum Disorder. *Eur. J. Med. Genet.* **54**, e516–e520 (2011).

130. A. C. EDENS, M. J. LYONS, R. M. DURON, B. R. DUPONT, K. R. HOLDEN, Autism in two females with duplications involving Xp11.22-p11.23. *Dev. Med. Child Neurol.* **53**, 463–466 (2011).

131. B. D. Semple, K. Blomgren, K. Gimlin, D. M. Ferriero, L. J. Noble-Haeusslein, Brain development in rodents and humans: Identifying benchmarks of maturation and vulnerability to injury across species. *Prog. Neurobiol.* **106–107**, 1–16 (2013).

132. B. Ye, N. Sugo, P. D. Hurn, R. L. Huganir, Physiological and pathological caspase cleavage of the neuronal RasGEF GRASP-1 as detected using a cleavage site-specific antibody. *Neuroscience*. **114**, 217–227 (2002).

133. P. Svenningsson *et al.*, Involvement of AMPA receptor phosphorylation in antidepressant actions with special reference to tianeptine. *Eur. J. Neurosci.* **26**, 3509–3517 (2007).

134. C. Yüksel, D. Öngür, Magnetic Resonance Spectroscopy Studies of Glutamate-Related Abnormalities in Mood Disorders. *Biol. Psychiatry*. **68**, 785–794 (2010).

135. J. Du *et al.*, The Anticonvulsants Lamotrigine, Riluzole, and Valproate Differentially Regulate AMPA Receptor Membrane Localization: Relationship to Clinical Effects in Mood Disorders. *Neuropsychopharmacology*. **32**, 793–802 (2007).

136. P. Svenningsson *et al.*, Involvement of striatal and extrastriatal DARPP-32 in biochemical and behavioral effects of fluoxetine (Prozac). *Proc. Natl. Acad. Sci. U. S. A.* **99**, 3182–7 (2002).

137. V. Szegedi *et al.*, Tianeptine potentiates AMPA receptors by activating CaMKII and PKA via the p38, p42/44 MAPK and JNK pathways (2011), doi:10.1016/j.neuint.2011.10.008.

138. J. Choi *et al.*, Phosphorylation of stargazin by protein kinase A regulates its interaction with PSD-95. *J. Biol. Chem.* **277**, 12359–63 (2002).

139. C. C. Chu *et al.*, Neurotrophic effects of tianeptine on hippocampal neurons: A proteomic approach. *J. Proteome Res.* **9**, 936–944 (2010).

140. T. Yamashima, Ca2+-dependent proteases in ischemic neuronal death. *Cell Calcium*. **36**, 285–293 (2004).

141. A. Das, M. K. Guyton, J. T. Butler, S. K. Ray, N. L. Banik, Activation of calpain and caspase pathways in demyelination and neurodegeneration in animal model of multiple sclerosis. *CNS Neurol. Disord. Drug Targets*. **7**, 313–20 (2008).

142. S. L. Williamson *et al.*, A novel transcript of cyclin-dependent kinase-like 5 (CDKL5) has an alternative C-terminus and is the predominant transcript in brain. *Hum. Genet.* **131**, 187–200 (2012).

143. E. Formstecher *et al.*, Protein interaction mapping: a Drosophila case study. *Genome Res.* **15**, 376–84 (2005).

Marco Tramarin
Laboratory of Genetic and Epigenetic Control of Gene Expression
Department of Biotechnology and Life Sciences
University of Insubria
Via Luciano Manara 7
21052 Busto Arsizio (VA), Italy